Woods Hole Oceanographic Institution

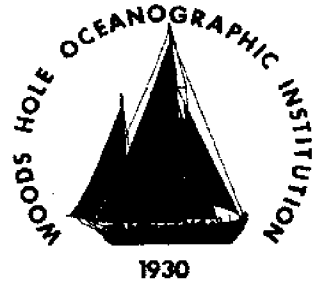

SHORT ARM ELECTRIC FIELD MEASUREMENTS OF OCEAN CURRENTS

by

Albert J. Williams III
Richard J. Jaffee
Peter F. Poranski
Paul J. Simonetti

February 1972

TECHNICAL REPORT

Prepared for the National Oceanic and Atmospheric Administration under Sea Grant No. 104 and ONR Contract N00014-66-C0241; NR 083-004.

Approved for public release, distribution unlimited.

WOODS HOLE, MASSACHUSETTS 02543

WHOI-72-13

SHORT ARM ELECTRIC FIELD MEASUREMENTS OF OCEAN CURRENTS

by

Albert J. Williams III[1]
Richard J. Jaffee[2]
Peter F. Poranski[2]
Paul J. Simonetti[2]

WOODS HOLE OCEANOGRAPHIC INSTITUTION
Woods Hole, Massachusetts 02543

February 1972

TECHNICAL REPORT

Prepared for the National Oceanic and Atmospheric Administration under Sea Grant No. 104 and ONR Contract N00014-66-C0241; NR 083-004.

Approved for public release, distribution unlimited.

Approved for Distribution E E Hays

E. E. Hays, Chairman
Department of Ocean Engineering

[1]Woods Hole Oceanographic Institution

[2]Woods Hole Oceanographic Institution and Massachusetts Institute of Technology Joint Program.

FOREWORD

Under support of the Office of Sea Grant Projects, the Woods Hole Oceanographic Institution conducts an educational summer program in oceanographic engineering. This program, in its second year, encompasses lectures on oceanographic instrumentation, seminars and lunchtime talks on oceanographic subjects. Additionally, student projects involving field and laboratory experience are performed. Four second year and two entering graduate students from the WHOI/MIT joint program in ocean engineering registered for the 1971 summer program. The results of their work appear as two reports to which this foreword is appended. Professor Robert L. Miller of the University of Chicago supervised and collaborated with Jay M. Cohen, Carl S. Albro, and James R. O'Sullivan on a study of sedimentation in Great Harbor (WHOI reference 72-12). I supervised and collaborated with Richard J. Jaffee, Peter F. Poranski, and Paul J. Simonetti in the construction and deployment of a towed geomagnetic-electro kinetograph (WHOI reference 72-13).

Albert J. Williams III
Assistant Scientist, WHOI

February 7, 1972

ABSTRACT

The construction of a bottom mounted electromagnetic current meter which would measure the vertically-averaged conductivity weighted horizontal velocity is necessary for the determination of the true horizontal velocity vector by electromagnetic techniques. A towed surface instrument which is the first prototype for the bottom mounted instrument was constructed and tested during the course of the summer. A salt bridge used in conjunction with a valve switching arrangement permitted the induced electromotive force and the electrode offset potential to be easily determined. Extensive laboratory tests and several field experiments proved the reliability and effectiveness of this design. Field tests included towing the instrument at the ocean surface and implantment of the instrument on the bottom in shallow water.

ACKNOWLEDGEMENTS

The successful completion of the project described here was due in part to the combined efforts of many of the W.H.O.I. staff. The authors wish to thank Dr. Thomas Sanford for his helpful advice and encouragement during the project. We wish to thank Mr. James Sullivan for his invaluable assistance in the fabrication of the instrument. We also wish to acknowledge Karen Pires for her excellent typing of the manuscript.

TABLE OF CONTENTS

Page No.

Abstract i

Acknowledgements ii

List of Illustrations. v

Introduction 1

A. Background of Motional Electric Field Measurements 2

I. Basic Physical Principles which Govern the Operation of the Geomagnetic Electro-Kinetograph. 2

1) Illustration of Electric Fields in the Sea by Means of Simple Physical Reasoning 2

2) Actual Electric Fields Measured by the GEK. 9

3) Analytic Relations for GEK Measurements 10

4) Remarks on GEK Use in Areas of Substantial Vertical Motion such as Tidal Currents Through Narrow Straits. . . 14

II. Previous Efforts and Devices Employed to Measure Flows in the Sea Using the Electromagnetic Method. 15

1) Brief Historical Outline. 15

2) Two Recent GEK Devices. 16

a) The Towed Electrodes of Von Arx (1950). 16

b) The Free-Fall GEK (Drever and Sanford, 1970). 21

B. Switched Electrode Geomagnetic Electro-Kinetograph 24

I. Instrument Description. 24

1) Operation 24

2) Fabrication 24

3) Electrodes. 29

4) Electronics 33

5) Pressure Sensor 38

6) Miscellaneous Equipment 40

TABLE OF CONTENTS (Cont.)

II. Instrument Problems and their Solutions 48

C. Laboratory and Field Tests of the Switched Electrode GEK, Both Towed on the Surface and Anchored on the Bottom 52

I. Shakedown Tests 52

1) Towed Tests 52

2) Bottom Tests. 54

II. Evaluation Tests. 54

1) Bottom Tests. 54

Appendix 1 74

Appendix 2 75

Bibliography 77

LIST OF ILLUSTRATIONS

		Page No.
Fig. 1	Conductor Moving in Magnetic Field	3
Fig. 2	Circuit Analogy for Homogeneous Ocean Moving in a Magnetic Field	3
Fig. 3	Electrical Current Density Lines for an Idealized Ocean Current	5
Fig. 4	Equivalent Circuit for Ocean Current in Fig. 3	6
Fig. 5	Circuit Analogy for a Stratified Ocean Moving in a Magnetic Field	8
Fig. 6	Towed GEK	10
Fig. 7	Typical Course to Eliminate Offset Potential	18
Fig. 8	Electrode Reversing Scheme	20
Fig. 9	Free-Fall GEK	21
Fig. 10	Free-Fall GEK Electrodes	22
Fig. 11	Salt Bridge Rotation	23
Fig. 12	Operational Diagram of Towed Surface GEK	25
Fig. 13	Block Diagram - Towed Surface GEK	26
Fig. 14	Summer Project Schedule	27
Fig. 15	Instrument - Cover On	30
Fig. 16	Instrument - Cover Off	31
Fig. 17	Silver Silver-Chloride Electrode	32
Fig. 18	Electrode Section Solenoids De-energized	34
Fig. 19	Electrode Section Solenoids Energized	35
Fig. 20	Electronics Section	36
Fig. 21	Electronic Amplifier Schematic	37
Fig. 22	Electrode Section	39
Fig. 23	End View of Instrument	41
Fig. 24	Front End of Instrument	42

LIST OF ILLUSTRATIONS (Cont.)

Fig. 25	Female Connectors and Eye Splice	43
Fig. 26	Eight Conductor Cable	44
Fig. 27	Winch	46
Fig. 28	PVC Housing	47
Fig. 29	Ground Loops Schematic	50
Fig. 30	Vertical Stand	53
Fig. 31	Course A-B August 13, 1971	57
Fig. 32	Course B-C August 13, 1971	58
Fig. 33	Course C-D August 13, 1971	59
Fig. 34	Course D-H August 13, 1971	60
Fig. 35	Typical Data ASTERIAS August 13, 1971	61
Fig. 36	Gates of Canso 1330-1730	64
Fig. 37	Gates of Canso 1730-2130	65
Fig. 38	Gates of Canso 2130-0130	66
Fig. 39	Gates of Canso 0130-0530	67
Fig. 40	Gates of Canso 0530-0800	68
Fig. 41	Typical Data - Gates of Canso Outgoing Flow	69
Fig. 42	Typical Data - Gates of Canso Incoming Flow	70
Fig. 43	Offset Potential Drift Gates of Canso 1330-2230	71
Fig. 44	Offset Potential Drift Gates of Canso 2230-0800	72
Table 1	Budget - Summer Project	28
Chart I	Course of ASTERIAS August 13, 1971 Vineyard Sound	56
Chart II	Gates of Canso August 17 and 18, 1971 Bottom Deployment	63

INTRODUCTION

The Geomagnetic Electro-Kinetograph (GEK) measures the electric fields induced in itself and in the sea due to motion through the earth's magnetic field. In all previous electromagnetic current meters a serious problem has been the determination of the offset potential of the electrodes in the sea water. The effect of this problem is to have limited the convenience and accuracy of some such current meters. The usefulness of other electromagnetic current meters, such as the free-fall GEK (Drever and Sanford, 1970), has been limited by the fact that $\overline{V}^*$ is an unknown, where $\overline{V}^*$ is the vertically-averaged conductivity weighted horizontal velocity in the entire water column. Since the free-fall GEK measures $V(z)-\overline{V}^*$, only the relative horizontal ocean currents as a function of depth can be determined. Thus, there is a strong need for the development of a bottom mounted GEK which would measure $\overline{V}^*$.

This summer a new type of towed surface GEK has been constructed which is the first prototype for the bottom mounted GEK. The problem of determining the electrode offset potential has been solved by a valve mechanism which switches the salt bridge connections to the electrodes.

This paper is divided into three parts: a discussion of the physical principles upon which the operation of the instrument is based, a description of the instrument itself, and an analysis of the data obtained from the instrument during the course of the summer.

SECTION A

Background of Motional Electric Field Measurements

I. Basic Physical Principles Which Govern the Operation of the Geomagnetic Electro Kinetograph (GEK)

The GEK is a device capable of continuously providing a detailed kinematic description of the mean and turbulent horizontal motions of the sea at a given depth or in profile from top to bottom. It accomplishes this task indirectly by measuring the electric fields induced in the sea water by the movements of this water through the geomagnetic field. The velocities of these water movements are rigidly related to the electric fields measured by the instrument through certain physical principles which are here presented.

1) ILLUSTRATION OF ELECTRIC FIELDS IN THE SEA BY MEANS OF SIMPLE PHYSICAL REASONING

The induced fields arise as a direct consequence of Faraday's Law of Magnetic Induction, which stated in words says that the EMF induced in a circuit moving with respect to a magnetic field is equal to the negative time rate of change of magnetic flux (ϕ_B) through the circuit.

In equation form this is:

$$EMF = -d\phi_B/dt$$

Consider a conducting bar of length D moving at a constant velocity V with respect to a uniform magnetic field B, which is directed into the paper as shown in Fig. 1.

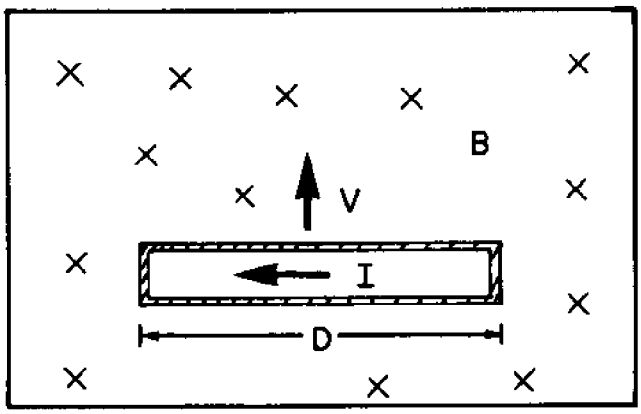

Figure 1. Conductor Moving in Magnetic Field

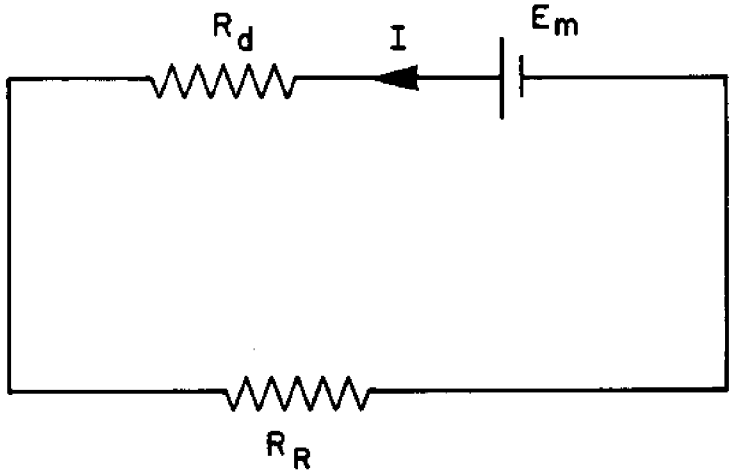

Figure 2. Curcuit Analogy For a Homogeneous Ocean Moving in a Magnetic Field.

In a certain time dt, the bar moves forward a distance dx. The magnetic flux $d\phi_B$ through the surface area swept by the bar during this time is

$$d\phi_B = BdxD$$

The time rate of change of flux and hence the induced voltage is equal to

$$|EMF| = |-\partial\phi_B/\partial t| = BDdx/dt = BDV$$

Lenz's Law demands that the current arising from this EMF flows from right to left as indicated in Fig. 1 in order that flux be decreasing in the area over which the bar has passed.

If the bar were electrically connected to some external resistance which is stationary with respect to the magnetic field, one would have a circuit which is a first crude analogy to the flow of electric current in response to motional electric fields in the ocean.

Sea water is a collection of highly ionized salts and hence an electrical conductor. If a horizontal ocean current having a rectangular cross-section of width D were flowing with a constant velocity V with respect to the vertical component of the earth's magnetic field F_z, it would produce effects similar to those associated with the previously mentioned conducting bar. That is, as it flowed it would generate a constant EMF proportional to VF_zD and the return circuit would be closed through the rest of the water column which was not in motion and the bottom sediments. In constructing a circuit analogy, the constant motional EMF and the moving water section are replaced by a battery E_m and a resistance R_d and the return circuit of motionless water and bottom sediments by a resistance R_R. The complete circuit is pictured in Fig. 2.

While this simplified circuit is crude in its approximation, it does serve to point up a few important aspects which are of interest in evaluating the results of any GEK experiments. Consider an idealized ocean current. Let its width be D and the depth of the water be designated as h. Lines of electrical current density J for this idealized stream would appear in the sea roughly as shown below in Fig. 3.

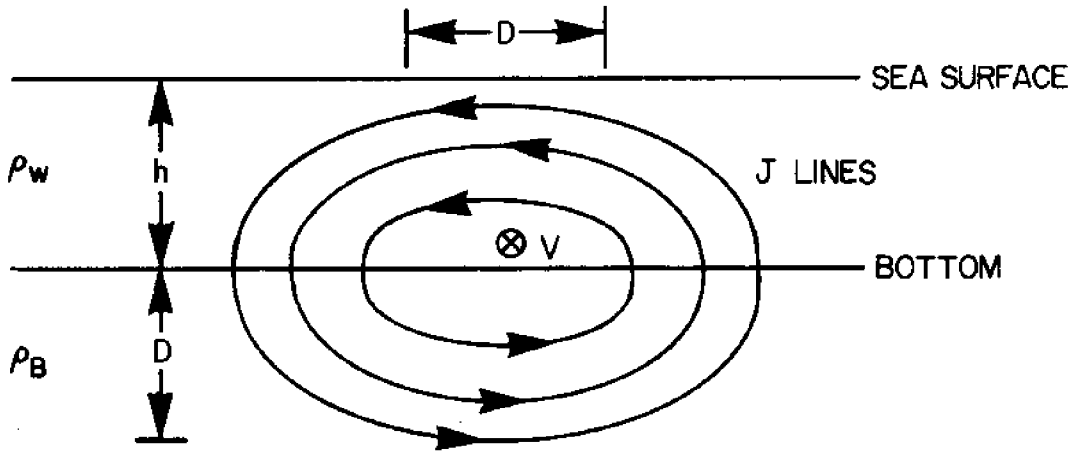

Figure 3. Electrical Current Density Lines For an Idealized Ocean Current.

Let the stream extend uniformly to the bottom and let the resistivity of the bottom and the water be ρ_B and ρ_w respectively.

The resistance R_D of the water will be approximately

$$R_D = \rho_w D/h$$

For such a stream, the electric current extends down into the bottom to a distance approximately equal to D, the width of the ocean current and hence R_B the bottom resistance is approximately

$$R_B = \rho_B D/D = \rho_B$$

The equivalent circuit for such a case is pictured in Fig. 4.

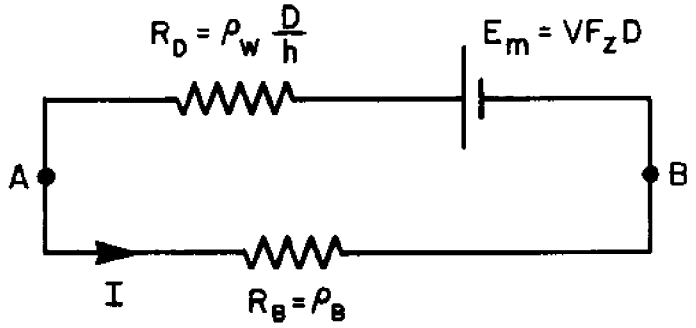

Figure 4. Equivalent Circuit For Ocean Current in Figure 3.

The electric current flowing around the circuit in Fig. 4 is

$$I = E_m/(R_D+R_B)$$

The potential difference between points A and B is given by

$$\phi_A - \phi_B = IR_B = \frac{E_B}{1+R_D/R_B}$$

or in terms of the physical parameters

$$\phi_A - \phi_B \simeq \frac{VF_z D}{1+\rho_w D/\rho_B h}$$

As will be seen later, an important quantity of interest in GEK studies is the horizontal component of potential gradient in the sea which is here roughly given by

$$|\nabla\phi|_H \simeq (\phi_A-\phi_B)/D \simeq \frac{VF_z}{1+\rho_w D/\rho_B h}$$

For a given flow at a certain place in the earth's magnetic field, $\nabla\phi$ is dependent on the ratio $\rho_w D/\rho_B h$. The quantity ρ_w/ρ_B can vary between unity and 2.5×10^{-5}. The quantity D/h is of course dependent on the cross-section of the flow itself. For a current such as the Gulf Stream, D/h is approximately 10. Thus the potential gradient can vary greatly depending on the shape of the flow and the electrical properties of bottom beneath it. In general, flow in the deep ocean does not extend to the bottom as the foregoing exercise has assumed but is instead confined to the upper layers. Thus the return circuit consists not only of the bottom but also

of the fairly large section of motionless sea water beneath the flow. The simplified circuit of Fig. 2 must thus be changed to correspond more fully with reality in the ocean. This can be accomplished by replacing the single battery E_m and resistor R_D with an array of n batteries E_{m_i} and series resistors R_{D_i} connected in parallel to represent the values of induced voltages and resistances at n levels in the ocean. Such a concept is shown schematically in Fig. 5.

Since the velocity profile in the ocean varies continuously with depth, n should approach infinity. The strength of the individual batteries E_{m_i} will now be $V_i F_z D$ where V_i is the flow velocity at the i^{th} level. Assuming that the sea water conductivity is constant with depth, each resistor R_{D_i} will have a resistance of $\rho_w D/dz$ as n approaches infinity. In this notation dz is the differential element of depth. Since $\phi_A - \phi_B$ is the potential difference between points A and B, the current flowing in each level dI_i will be given by

$$dI_i = \frac{dz}{\rho_w D} (\phi_A - \phi_B - V_i F_z D)$$

The total current I in the n levels is given by

$$I = \frac{1}{\rho_w D} \int_{-h}^{o} (\phi_A - \phi_B - V_i F_z D) dz$$

$$= \frac{h}{\rho_w D} (\phi_A - \phi_B - \overline{V} F_z D)$$

where $\overline{V}$ is the vertically averaged velocity

$$\overline{V} = \frac{1}{h} \int_{-h}^{o} V_i dz$$

It is thus seen that the n levels of batteries and resistors is equivalent to a single battery of voltage $\overline{V} F_z D$ in series with a resistor $\overline{R}_D = \rho_w D/h$.

For ocean currents where flow is confined to the near surface waters, the batteries near the bottom (E_{m_i} where i is large) are of zero value.

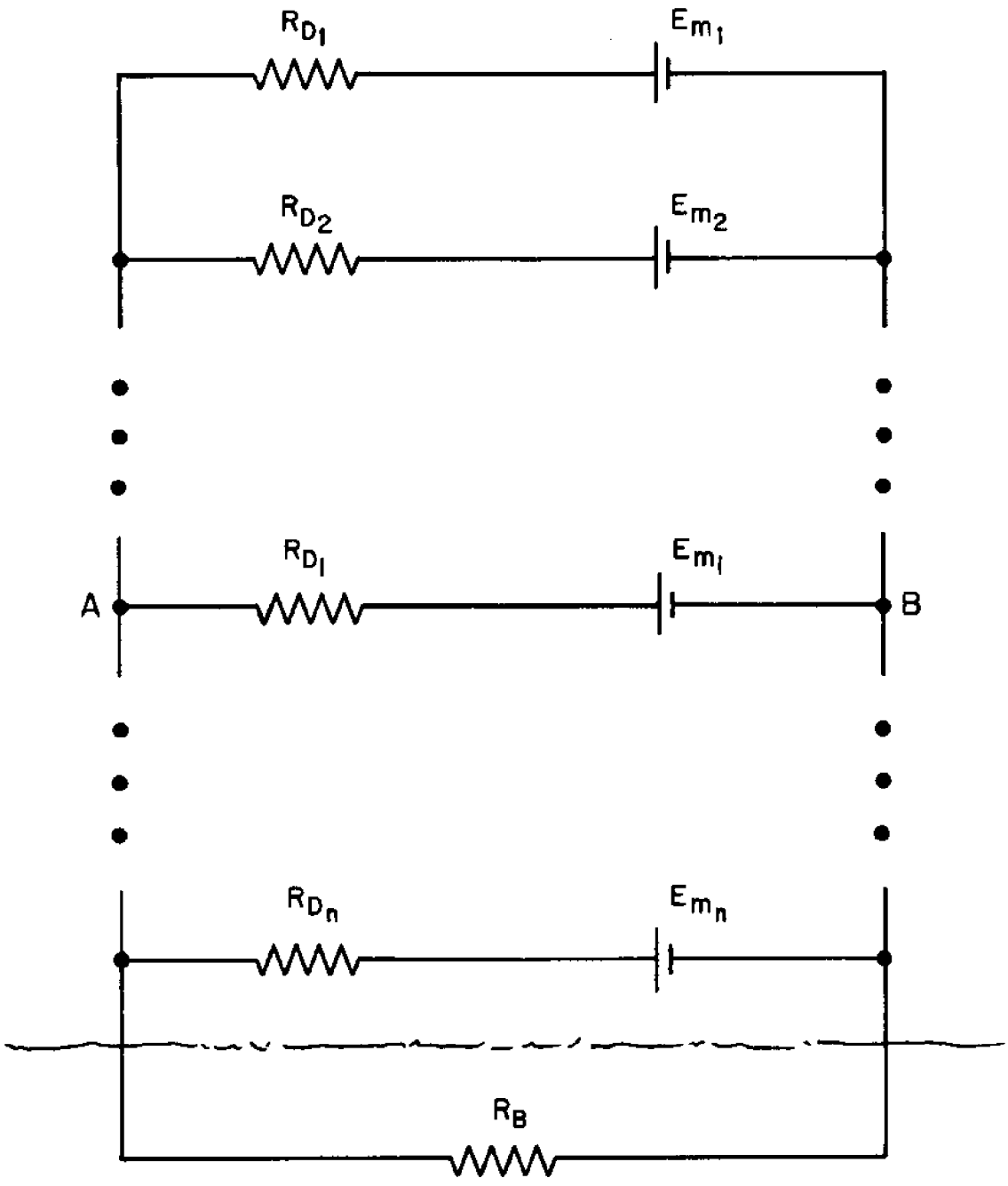

Figure 5. Circuit Analogy For a Stratified Ocean Moving in a Magnetic Field.

In trying to measure any E_{m_i} by means of a GEK, it would be desirable to minimize the voltage developed in the return circuit through the levels of motionless water and the bottom. This is accomplished if the return shunt resistance R_R of these areas is small where

$$1/R_R = z/\rho_w D + 1/R_B$$

and z is the thickness of motionless water.

It is thus seen that R_R will be least for largest z. The condition of large z is most often found in open ocean currents where the flow is largely confined to the top levels near the surface, and it is here that the GEK technique finds its best use.

One might very well ask why the various parallel branches of the circuit are not connected by some resistances in the vertical direction instead of with short circuits as pictured in the schematic of Fig. 5. Let such a resistance be denoted as R_{V_i} where $R_{V_i} = \rho_w dz/D$. Then the total vertical resistance $\overline{R}_V$ is given by $\overline{R}_V = \int_{-h}^{o} \rho_w dz/D = \rho_w h/D$, so that $\overline{R}_V/\overline{R}_D = h^2/D^2$.

For a current like the Gulf Stream with an approximate width of 50 km. and in a depth of 5 km. of water, the ratio is $\overline{R}_V/\overline{R}_D = 5^2/50^2 = 1/100$.

Hence $\overline{R}_V$ can be neglected for most work in large scale ocean currents.

2) ACTUAL ELECTRIC FIELDS MEASURED BY THE GEK

Returning again to the simple circuit of Fig. 2, Kirchoff's Law around it yields $E_m - IR = 0$ where $R = R_D + R_R$.

For a sea water segment, this statement of Ohm's Law is more conveniently written in terms of the gradient of the electrostatic potential in the sea $\nabla\phi$, the induced electric field vector $\vec{E}$, and the current density $\vec{J}$ as

$$\vec{E} - \vec{J}/\sigma = \nabla\phi$$

where σ is the conductivity of the water segment.

For the sea water segment as with the moving conducting bar of Fig. 1, the induced electric field is equal to $\vec{E} = \vec{V}x\vec{F}$ where $\vec{V}$ is the vector velocity of the water segment relative to $\vec{F}$, the earth's magnetic field vector.

Since the GEK pertinent to this report is usually towed, a few words about what quantities are actually measured during such a procedure are in order. (The following also applies to the vertical free-fall GEK which is in a sense "towed" in reverse by being advected by the horizontal velocity of the current it is falling through. The operation of this instrument will be described later in another section.)

3) ANALYTIC RELATIONS FOR GEK MEASUREMENTS

Fig. 6 shows a ship moving with velocity $\vec{V}_s$ with respect to the water and the towed GEK streaming behind. $\vec{V}$ is the velocity of the water with respect to the earth at the level of the instrument.

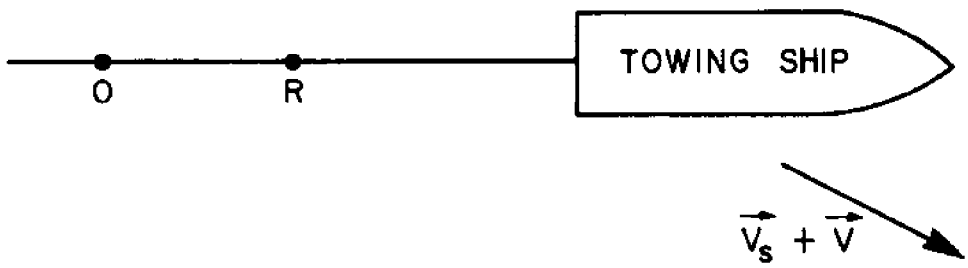

Figure 6. Towed GEK

The distance $\overline{OR}$ can either be an interelectrode distance as in earlier GEK's or it can be the length of salt bridge which is attached to the instrument in the present study.

In the absence of sideways disturbances, the absolute velocity of the segment $\overline{OR}$ equals the absolute velocity of the ship which is

$$\vec{V}_{\overline{OR}} = \vec{V}_s + \vec{V}$$

The voltage measured in $\overline{OR}$ will consist of two terms: the voltage in the sea between points O and R, minus the voltage induced in $\overline{OR}$ by virtue of its motion through the magnetic field of the earth.

Thus,

$$(\text{Voltage})_{\text{measured}} = [\nabla\phi - (\vec{V}_s + \vec{V})\times\vec{F}]\cdot\overline{OR}.$$

However, $\vec{V}_s \times \vec{F}$ is perpendicular to $\overline{OR}$ and hence

$$(\vec{V}_s \times \vec{F})\cdot\overline{OR} = 0.$$

Therefore, the voltage measured by a towed GEK will be

$$(\text{Voltage})_{\text{measured}} = (\nabla\phi - \vec{V}\times\vec{F})\cdot\overline{OR}.$$

This says that the measured voltage is independent of the towing velocity of the ship once a state has been reached in which there are no sideways or up and down disturbances acting on the line containing $\overline{OR}$.

Since $\nabla\phi = \vec{V}\times F - \vec{J}/\sigma$, the measured voltage may be written as

$$(\text{Voltage}) \text{ measured} = (-\vec{J}/\sigma)\cdot\overline{OR}$$

and hence the towed GEK measures the component of electric current density $-\vec{J}/\sigma$ in the direction of the towed line $\overline{OR}$.

This is an important result for it now tells the GEK user exactly what he is measuring, which in terms of the measured electric field is,

$$\vec{E}_{\text{measured}} = -\vec{J}/\sigma = (\nabla\phi - \vec{V}\times\vec{F}) = -(\vec{V}\times\vec{F} - \nabla\phi).$$

In the above relation, the item of oceanographic interest is of course $\vec{V}$, the current velocity. Values of $\vec{F}$ are readily available from tables and if the components of $\nabla\phi$ were known, $\vec{V}$ could be found by measuring the voltage $(-\vec{J}/\sigma)\cdot\overline{OR}$ on two courses at an angle to each other and transforming these vectors to determine $\vec{V}$, the horizontal current velocity vector. However $\nabla\phi$, the gradient of electrostatic potential in the sea, is not initially known and so the measured voltage, and hence the calculated current $\vec{V}$, is deficient by a factor.

From the earliest GEK operations, it became necessary to cope with the lack of knowledge about the value of potential gradient ($\nabla\phi$) in the sea, in order to calculate current velocities from GEK measurements. Thus it became

expedient to define a "K" factor which is equal to

$$K = \frac{|\vec{V}x\vec{F}|}{|(\vec{V}x\vec{F})-\nabla\phi|} \quad .$$

Thus the K factor is simply the ratio of the desired or expected signal $(\vec{V}x\vec{F})$, from which the current velocity $\vec{V}$ may be directly calculated, to the actual signal received which contains the troublesome quantity $\nabla\phi$ about which nothing could be said. The K factor in effect is proportional to the strength of the potential gradient in the sea $\nabla\phi$. As was previously seen in the rough physical arguements pertaining to the sea water-bottom equivalent circuit of Fig. 4, $\nabla\phi$ roughly depends on the ratio of the sea water to bottom resistivities, the width of the current and the depth of the water. The K factor for a particular area of the sea was either estimated from a knowledge of these factors in the locale or calculated from the ratio of water speeds observed by non-electromagnetic and magnetic devices. The average open sea value of K was placed at 1.04 whereas on the continental shelf it averages less than 2.0 and in shoal water may range from 1.5 to 15.0. Once a K factor had been decided upon for a particular set of data, the signal received $[-(\vec{V}x\vec{F}-\nabla\phi)\cdot\overline{OR}]$ and the calculated velocity was then scaled up by a factor of K to give its "true" value. Even though results of such calculations were an important breakthrough for electromagnetic method, the continued use of such a quantity was to perpetuate one of those nasty, empirical factors, lacking both aesthetic and scientific elegance. Moreover, it served to point out a fundamental lack of knowledge about an important quantity in the sea, namely $\nabla\phi$, the gradient of electrostatic potential existing there.

Recently, Sanford [1971] has analytically solved for the quasi-static electric field in the sea for an idealized model of the ocean and earth. His analysis shows that in an ocean current which is broad compared with

the ocean's depth, the potential gradient is independent of depth and a function of $\vec{\overline{V}}_H$, the vertically-averaged horizontal velocity in the entire water column. The horizontal components of the potential gradient in the sea are given by

$$\frac{\partial \phi}{\partial_x} = F_z \overline{V}_y$$

$$\frac{\partial \phi}{\partial_y} = -F_z \overline{V}_x^* \qquad \text{where}$$

$$\vec{\overline{V}}^* = \frac{1}{D(1+\alpha)} \int_{-D}^{0} \vec{V}_H dz \qquad \text{and}$$

D = water depth

$\vec{V}_H = (V_x, V_y, 0)$

α = ratio of the conductance of bottom sediments to that of the ocean.

With this in mind a new expression for the actual electric field measured by the GEK technique may now be put forth. Recalling that

$$\vec{E}_{measured} = -\vec{J}/\sigma = -(\vec{V} \times \vec{F} - \nabla\phi)$$

where $\vec{V} = (V_x, V_y, 0)$

and $\vec{F} = (0, F_y, F_z)$,

the components of $\vec{E}_{measured}$ are

$$E_{measured\ x} = -F_z(V_y - \overline{V}_y^*)$$

$$E_{measured\ y} = F_z(V_x - \overline{V}_x^*)$$

These expressions say that if the x and y components of the measured electric field are found, the horizontal components of the absolute water velocity (V_x, V_y) at any given level, can be calculated if $\overline{V}_x^*$ and $\overline{V}_y^*$, the conductivity weighted, vertically averaged components of horizontal velocity, are known. One might think that this leaves the GEK user in no better position

than before since $\overline{V}_x^*$ and $\overline{V}_y^*$, like the potential gradient $\nabla\phi$, are initially unknown. However, unlike the potential gradient, $\overline{V}_x^*$ and $\overline{V}_y^*$ may be readily measured.

Consider a GEK device mounted on the bottom of the sea where both

$$V_x = 0$$

$$V_y = 0 \quad .$$

Thus the components of electric field measured by such an instrument would be

$$E_{\text{measured } x} = F_z \overline{V}_y^*$$

$$E_{\text{measured } y} = F_z \overline{V}_x^* \quad ,$$

and so $\overline{V}_x^*$ and $\overline{V}_y^*$ are easily determined in terms of the measured electric field. If now a towed GEK were concurrently deployed over the same site, the components of horizontal velocity could then be calculated since $\overline{V}_x^*$ and $\overline{V}_y^*$ would be known. Therefore the motivation for a bottom mounted GEK design is very acute as it would allow current velocities to be calculated in a way consistent with theoretical analysis and would further free the electromagnetic method from the empiricism which necessarily marked its early development.

4) REMARKS ON GEK USE IN AREAS OF SUBSTANTIAL VERTICAL MOTION SUCH AS TIDAL CURRENTS THROUGH NARROW STRAITS

All aspects of the previous analysis have assumed that the vertical component of current velocity V_z has been small enough to be neglected. This is very well justified for the open sea which is much wider than its depth but in narrow, violently flowing passages over an irregular bottom, substantial short-term vertical motions often occur. This may lead to an erroneous value for the horizontal velocity vector in the following way. Taking into account the vertical component of velocity V_z, a GEK device would see the following components of electric field.

$$E_x = -F_z(V_y - \overline{V}_y^*) + F_y V_z$$

$$E_y = F_z(V_x - \overline{V}_x^*)$$

Thus the x component of electric field has a term $F_y V_z$ due to the vertical component of current velocity which could be significant in certain shoal areas. Also the value of the potential in the water in such an area is not clear and hence the physics must again be looked at for a true attempt at a realistic measurement.

II Previous Efforts and Devices Employed to Measure Flows in the Sea Using the Electromagnetic Method

In order to better appreciate the workings of the particular instrument which is the subject of this report, it seems wise to review the efforts of others who have suceeded in the use of this method of measurement. A brief historical outline will first be presented in order to both show a progression in the ways people have measured induced electric fields in the past, and to illuminate some of the major problems encountered in previous devices. Following this, two recent GEK instruments will be examined in some detail in order to better pave the way for a comparison with the present instrument as a working piece of hardware.

1) BRIEF HISTORICAL OUTLINE

Michael Faraday, who discovered the laws of electromagnetic induction, was the first to predict the presence of induced electric fields in sea water. Not having been hamstrung by the rigid thinking resulting from years of formal education, this great geometrical thinker could easily picture a moving segment of sea water cutting the lines of force of the earth's magnetic field as easily as he saw a wire loop cutting those of a bar magnet (itself quite a feat). However, when Faraday set out to measure the induced fields across the Thames River, he discovered one of the single most important effects in the operation of any type of GEK

device; one which must be suppressed if the technique is to yield meaningful results at all. He found that when he placed copper electrodes opposite each other across the river, there developed at each electrode an offset or bias potential by virtue of the fact that the copper electrode and the river water formed a metal-electrolyte junction. If the copper electrodes were of identical physical properties and the two sections of water they were immersed in were the same in every conceivable way, then the two offset potentials would be equal and opposite and buck each other out. However, such conditions are unlikely at any time and hence the induced potentials which Faraday sought to measure were obscured by the offset which was much larger than the expected signal. The suppression of electrode bias cannot be ignored and will be encountered again in a later section when investigating recent GEK instruments as well as the present instrument under study.

After Faraday's effort, electromagnetic effects in the sea were observed on long lengths of broken telegraph cable after the middle of the 19th century. Serious scientific investigation began in 1918 when Young, Gerrard and Javons (1920) measured voltages induced by tidal motions in Dartmouth Harbor by means of moored and drifting electrodes.

In more recent times further measurements using submarine cables have been done by Stommel (1954) and Runcorn (1964). However, in relation to the present instrument under study, it is well to look at two recent GEK devices so as to see common problems inherent in all such devices and different methods of operation and measurement.

2) TWO RECENT GEK DEVICES

A.) The Towed Electrodes of von Arx (1950)

This device was the first of the GEK devices and consisted of two towed electrodes situated a few tens of meters apart on a two conductor

cable and a potentiometer attached to a strip chart recorder to register the measured signal on board the towing ship. Since the voltage measured along the electrode line is proportional to the component of the current velocity perpendicular to this line, two measurements at right angles to each other will determine two orthogonal velocity components from which their vector sum, the surface current vector, may be composed. The geographical direction of the currents can of course be determined by noting the headings on the ship's compass for each component measurement. Currents calculated from data gathered by this instrument were obtained using the K factor previously mentioned. Each electrode was housed in a strong formica cylinder (fitted with rounded end caps) through which the two conductor cable was passed and to which it was clamped. The electrode was housed inside the formica tube in a chamber filled with tightly packed glass wool. Electrical contact was made with the sea through holes drilled in the formica case which allowed water to enter the chamber and contact the electrodes.

Tests have found that silver-silver chloride electrodes are the type best suited for use in a GEK instrument. However even the most careful construction and attempts at matching cannot produce an electrode pair of identical properties. Furthermore, values of salinity, pressure, temperature, aeration, and other factors, and the time rates of change of these quantities are in general not the same at the two sites of the physically separated electrodes. All of these factors all contribute to mean that at each electrode, bias or offset potentials (and time drifts in these potentials) of the same type which hampered Faraday in his measurements on the Thames River, will appear. The towed electrode GEK of von Arx deals with this problem in the following ways.

From the foregoing discussion it is obvious that the voltage measured by the potentiometer on deck will consist of two parts: the difference between the offset potentials of the two electrodes and the motionally induced voltage, the desired signal.

Thus,

$$E_{measured} = (E_2-E_1)+E_{induced}$$

where E_1 and E_2 are the total offset potentials developed at electrodes 1 and 2 respectively. Since the offset difference cannot be eliminated, it would be helpful to at least be able to measure its value and subtract it out of the measured potential to yield the desired induced voltage.

One way to accomplish this is by means of a towing course for a GEK measurement like the one indicated in Fig. 7.

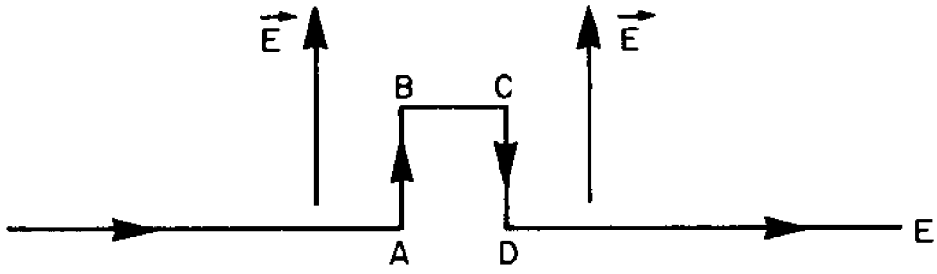

Figure 7. Typical Course to Eliminate Offset Potential.

Once the unit had been deployed and streaming properly, a 90° turn would be made at a point such as A. From A to B the deck recorder would measure a voltage of

$$E_{measured\ \overline{AB}} = (E_2-E_1)+E_{induced\ \overline{AB}} \quad .$$

At point B, at 180° turn indicated by the distance $\overline{BC}$ is made. The voltage measured from C to D is

$$E_{measured\ \overline{CD}} = (E_2-E_1)+E_{induced\ \overline{CD}} \quad .$$

If the distance $\overline{BC}$ is small, the ocean current normal to $\overline{AB}$ can be expected to be for all intents equal in magnitude and direction to that normal to $\overline{CD}$. Therefore, the electric fields induced in the sea by these velocities will

be equal in magnitude and direction (parallel to both $\overline{AB}$ and $\overline{CD}$) in both of these segments. However, in $\overline{CD}$ the positions of the two electrodes relative to these fields is 180° opposite to their position in $\overline{AB}$. Therefore, the induced voltage measured by the electrode pair along $\overline{AB}$ will be equal in magnitude but opposite in sense to that along $\overline{CD}$. Thus,

$$E_{\text{induced } \overline{AB}} = -E_{\text{induced } \overline{CD}}$$

and

$$E_{\text{measured } \overline{CD}} = (E_2-E_1)-E_{\text{induced } \overline{AB}} \quad .$$

Combining the total measured voltages along each leg and solving for the offset difference,

$$(E_2-E_1) = \frac{E_{\text{measured } \overline{AB}}+E_{\text{measured } \overline{CD}}}{2}$$

This point may be identified on the recording of the data and the measured potential with respect to this value is E_{induced}, the desired quantity. E_{induced} may be measured this way along the segment $\overline{DE}$ [assuming the offset (E_2-E_1) remains constant during that time] until point E is reached and the offset difference is determined again and so on at given intervals. Another advantage of such a towing course is that it allows the current vector to be periodically determined since orthogonal values of the induced voltage (and hence orthogonal components of current velocity) are obtained whenever a 90° turn is executed.

However, frequent course changes can be troublesome and serve to delay the ship. If considerations of this nature are important, another method of dealing with the offset potentials can be used. If the electrodes are switched in position 180° to the induced electric field as before without changing the course of the ship, the offset difference (E_2-E_1) can be determined in the same way as the previous scheme but without ship delay. A plan as pictured in Fig. 8 is used.

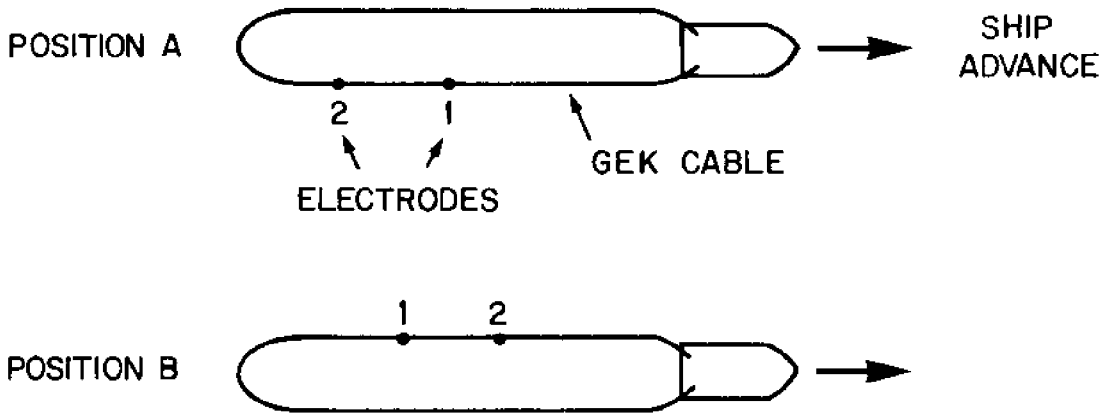

Figure 8. Electrode Reversing Scheme.

Measurements are taken in position A for a time and then the wire attached to the farthest electrode astern is hauled in while the GEK cable is held stationary. When the two electrodes are approximately the same distance astern, the wire line is held stationary and the GEK cable is paid out till the electrode positions have reversed end for end as seen in Position B of Fig. 8. Thus the offset may be determined in the same way as the previous towing plan while here the ship remains undeflected from its course. However, since orthogonal components of velocity cannot be computed without a 90° course change, the current velocity vector cannot be determined with such a scheme. A compromise is to physically reverse the electrodes along a zig-zag course over which velocity components can be found.

The first GEK device proved a success for the electromagnetic method and also served to show where areas for concentration were for future such devices. First, to avoid the effect on the offset potential of variations in temperature, salinity, airation, etc., at each electrode site, it seemed

desirable to place the electrodes closer together and yet keep the induced voltage (which is proportional to interelectrode distance), high.

Second, it would have been well if the offset potentials could be measured by future GEK's in some manner intrinsic to the device rather than by external means such as physical electrode reversal or course changes. Third, while the towed electrodes measure the horizontal velocity at a given level near the surface, an electromagnetic device to measure horizontal velocity in profile from top to bottom was also to be sought after. A more recent instrument which helps to answer some of these challenges will next be described.

B.) The Free-Fall GEK (Drever and Sanford, 1970)

The free-fall GEK copes with the serious matter of the electrode offset potentials in an ingenious way while providing a vertical profile of the shear in horizontal velocity in the deep sea in a rapid time. The instrument, shown below, is allowed to fall freely (1.25 m/sec) and the four constant-pitch fins cause the instrument to rotate at approximately 0.15 Hz as it falls. (See Figure 9)

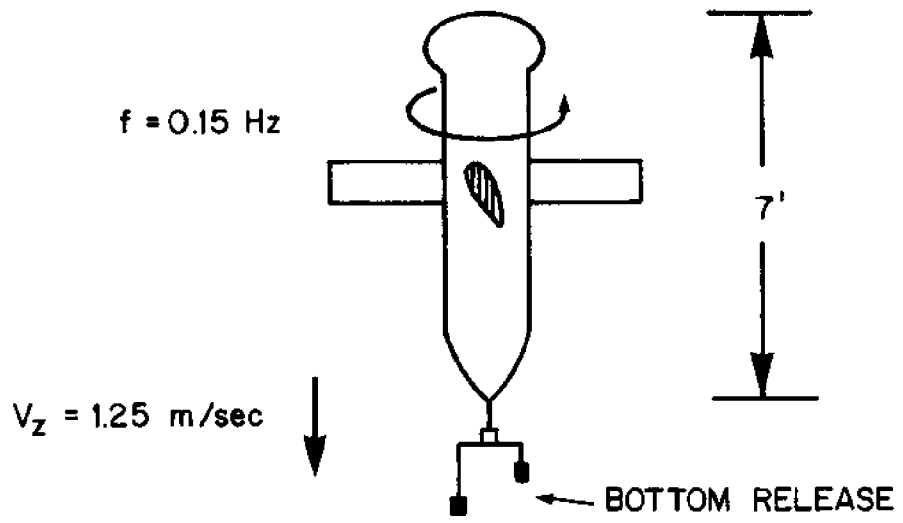

Figure 9. Free-Fall GEK.

Inside two opposing fins is a salt bridge in which two electrodes are mounted as displayed in Figure 10.

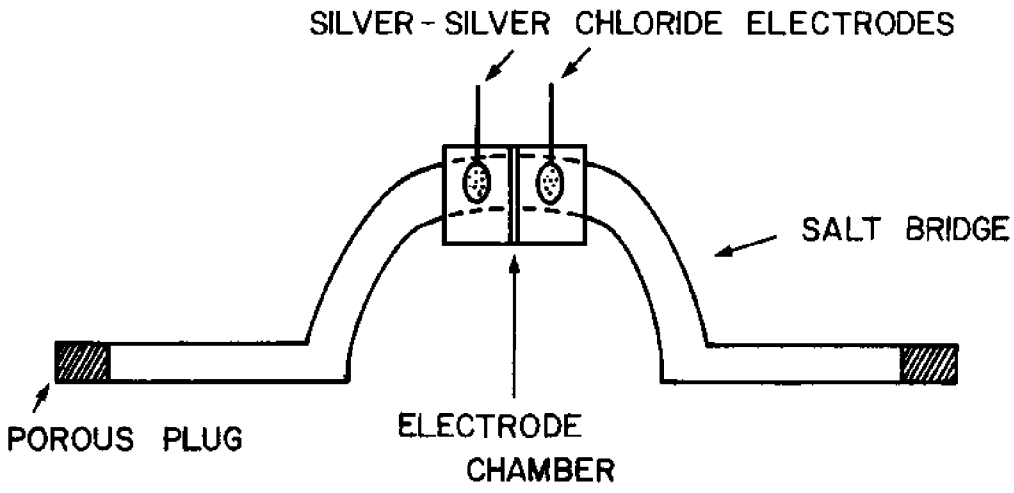

Figure 10. Free-Fall GEK Electrodes.

The porous plugs prevent air and dirt from entering the sea water in the arms of the salt bridge while providing a good electrical connection with the sea.

Again, as with the towed GEK, this device measures an apparent electric field $\vec{E}_m$, equal to

$$\vec{E}_m = -(\vec{V}x\vec{F}) + \nabla\phi \quad .$$

Now, however, the vertical fall speed of the instrument V_z is significant, and must be considered. Thus the components of the measured electric field are

$$E_{m_x} = -[F_z(V_y - \overline{V}_y^*) - F_y V_z]$$

$$E_{m_y} = F_z(V_x - \overline{V}_x^*) \quad .$$

In these equations it is assumed that the speed of vertical ocean currents is insignificant compared with the vertical fall speed of the instrument. However, since the salt bridge arms are spinning, they will at an arbitrary instant of time be aligned with the components of the induced field as such,

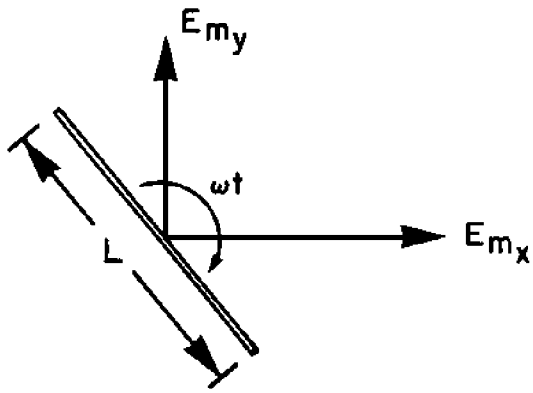

Figure 11. Salt Bridge Rotation.

where time t = 0 when L points North, and L is the length of the salt bridge. Therefore, the measured induced voltage will be time varying:

$$(\text{Volt})_{\text{measured}} = -[Fz(V_y - \overline{V}^*_y) - F_y V_z]L \sin wt + F_z(V_x - \overline{V}^*_x)L \cos wt$$

$$w = \text{angular frequency} = 2\pi(.15) \text{ rad/sec.}$$

The term involving $F_y V_z$ is of no interest since V_z, the vertical speed of the instrument, is known and can be cancelled out of the measurement by a suitable technique. The signal may then be written as

$$(\text{Volt})_{\text{measured}} = -F_z|V_H - \overline{V}^*| \sin (wt-\theta)$$

where θ is the direction of V_H with respect to North. Again, the signal received only enables the absolute horizontal velocity V_H to be determined with respect to the quantity $\overline{V}^*$ which must be found by another means such as a bottom mounted GEK instrument.

Only the alternating voltage is amplified and telemetered to the support vessel (here by acoustic means) so the signal consists only of the measured induced voltage while the large, undesirable potentials due to electrode bias and temperature and salinity differences at individual electrodes is ignored.

SECTION B

Switched Electrode Geomagnetic Electro-Kinetograph

I. Instrument Description

1) OPERATION

The unique design aspect of the surface GEK described in this paper is a valve switching arrangement which permits easy and efficient determination of the electrode offset potential. The two electrodes are mounted only three inches apart in a manifold inside the instrument. A solenoid operated valve which is normally closed separates the electrodes. A second solenoid operated valve which is normally open permits a sea water path between one of the electrodes and the sea near the case of the instrument. Figure 12 shows a schematic diagram of the surface GEK in normal operation. When the solenoids are both turned on, the valves connect the electrodes with a seawater short circuit and thus the electrode offset potential appears between them. This offset potential can then be subtracted from the signal obtained in normal operation to realize the true signal.

A schematic block diagram of how the surface GEK works is shown in Figure 13. It is seen that surface support is essential to the operation of the instrument. External power is needed to operate the solenoids and the electronics, while the analog electrode and pressure output signals must be recorded at the surface. For the proposed bottom GEK, these functions would have to be performed internally within the instrument.

2) FABRICATION

At the commencement of the project the design of the surface GEK had been completed by Dr. Williams. In addition the electrode manifold had been constructed with the solenoids, valves, and tubing emplaced. The final

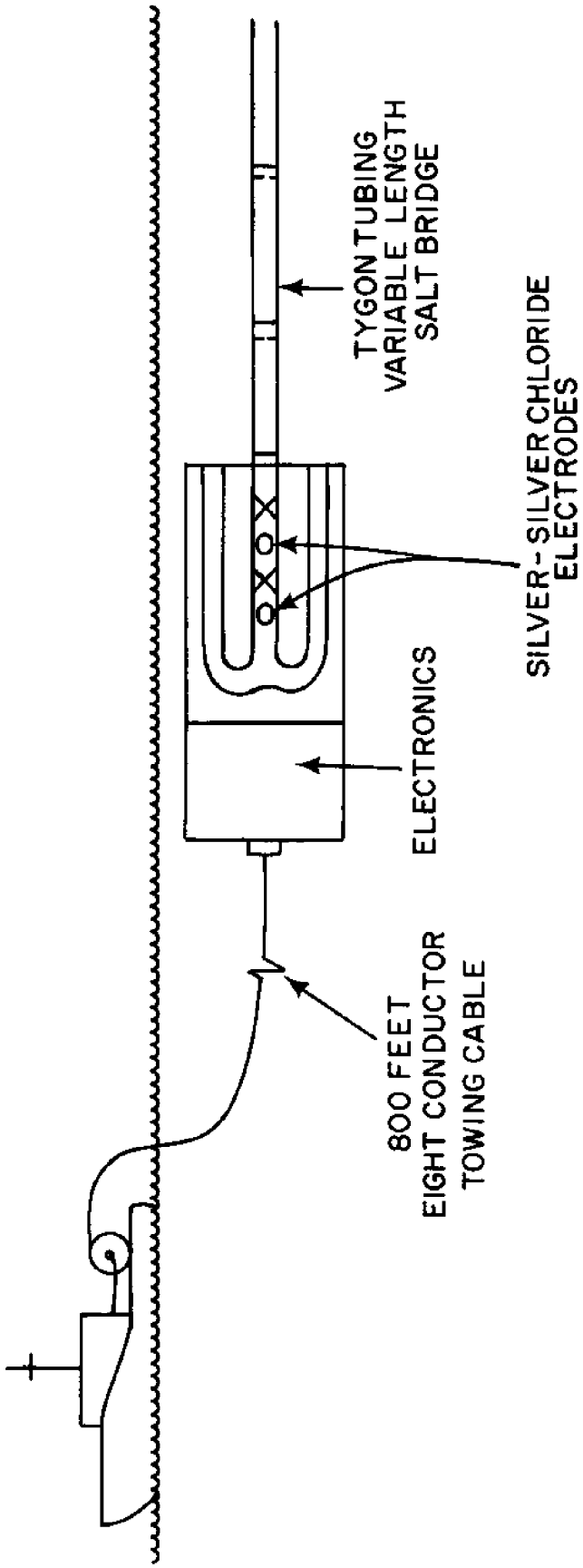

Figure 12. Operational Diagram of Towed Surface GEK.

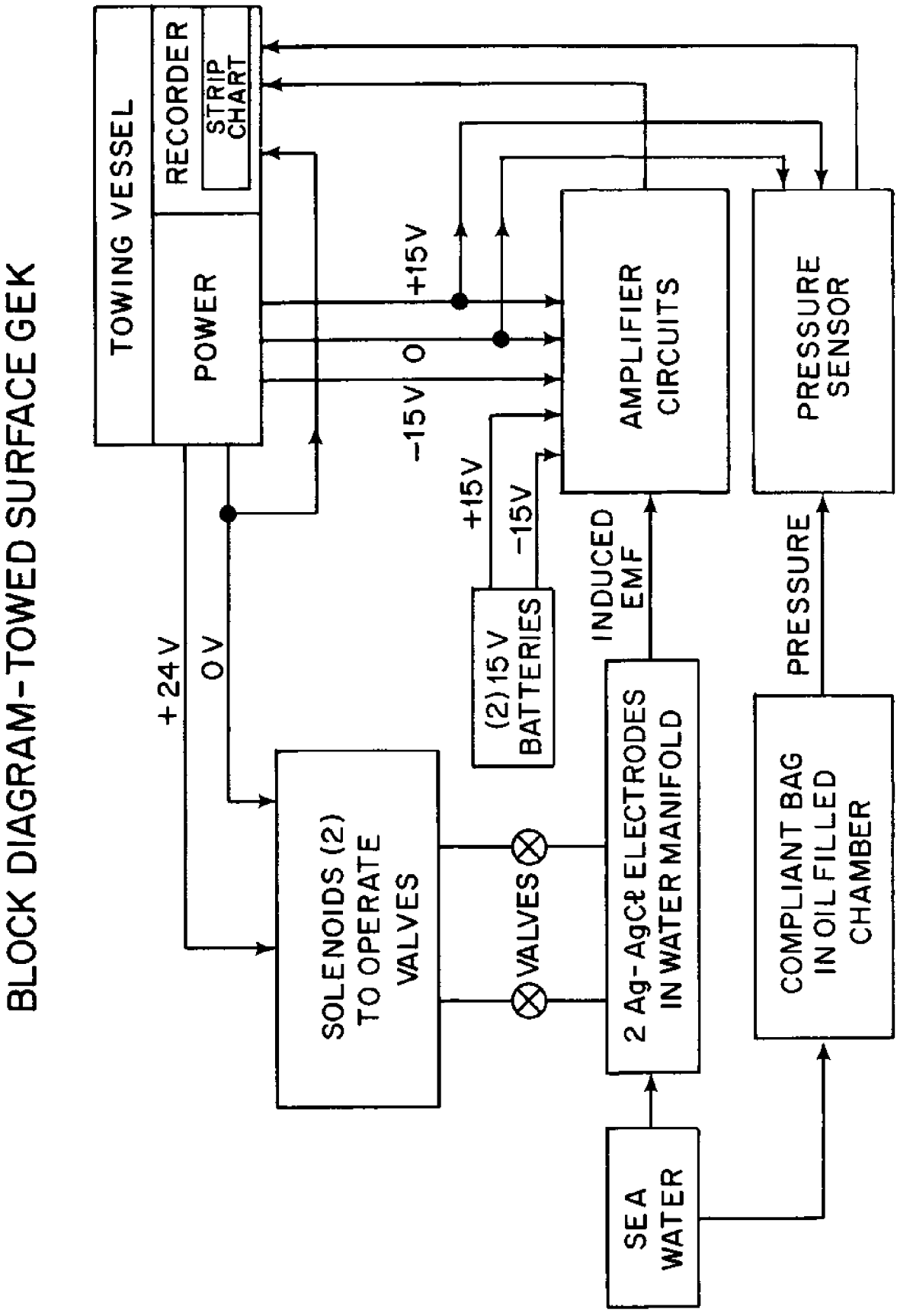

Figure 13. Block Diagram - Towed Surface GEK.

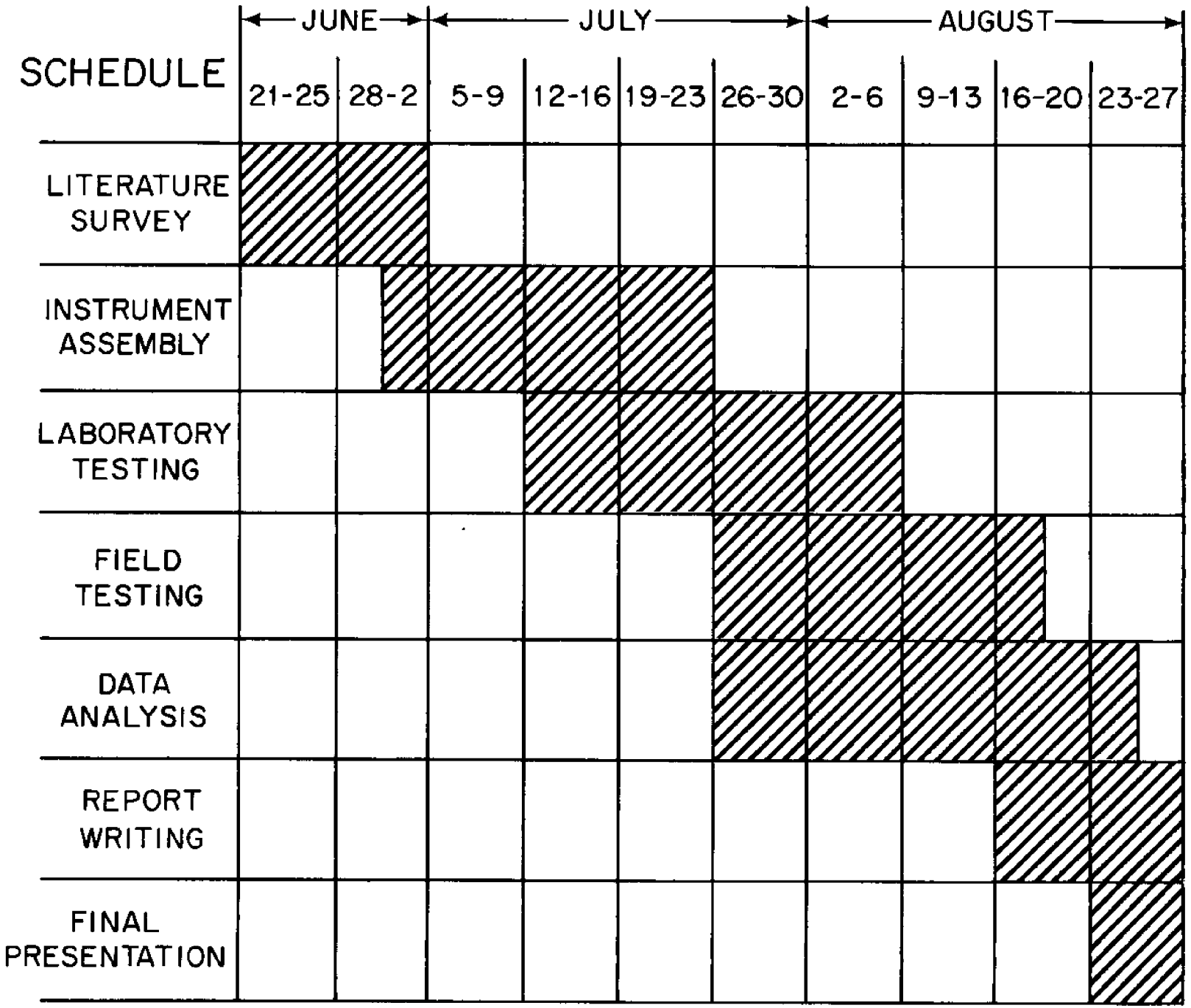

Figure 14. Summer Project Schedule.

Table 1. Budget - Summer Project.

Ship-time (ASTERIAS) three 1/2 days @ $53/1/2 day =	159.00
Batteries	75.00
Vertical Stand	40.00
Electronic Components	12.00
Wire, Cable, Rope	30.00
Final Assembly	30.00
Miscellaneous	25.00
	$ 371.00

assembly of the surface GEK which included construction of the electronics and integration of all connectors, fasteners, and miscellaneous parts took approximately 4 weeks. Laboratory and field testing of the instrument each took approximately 4 weeks as well, but each phase overlapped the previous phase. Figure 14 shows the schedule that was followed during the course of the summer. The project budget for the summer is shown in Table 1.

The instrument is approximately 2 feet long and weights 32 pounds in air. It is shown with and without its polyvinyl chloride (PVC) housing in Figures 15 and 16. In operation, the electrode section is oil filled and pressure compensated while the electronics section is air filled and pressure protected. The pressure sensor, located in the electronics section, monitors the oil pressure of the pressure compensated electrode section.

3) ELECTRODES

Figure 17 shows a picture of one of the silver-silver chloride electrodes before it was put into the electrode manifold. In the electrode manifold the electrodes are placed close to each other to minimize the temperature and salinity differences between them. A one degree centigrade temperature difference between the two electrodes causes an offset voltage of about 350 microvolts between the electrodes. A salinity difference of one part per thousand in the water near each electrode causes a voltage difference of about 500 microvolts, (Drever and Sanford, 1970). Thus, keeping the electrodes in close proximity, immersed in approximately the same water, reduces the offset potential between them. Although the electrodes are close to each other, they measure the potential between the ends of a salt bridge. The salt bridge consists of sea water filled tubes extending from each electrode. One conductive path extends from inside the GEK out to the end of a sea water filled Tygon tube, tens of meters away, while the other extends just out to the end of the instrument. The

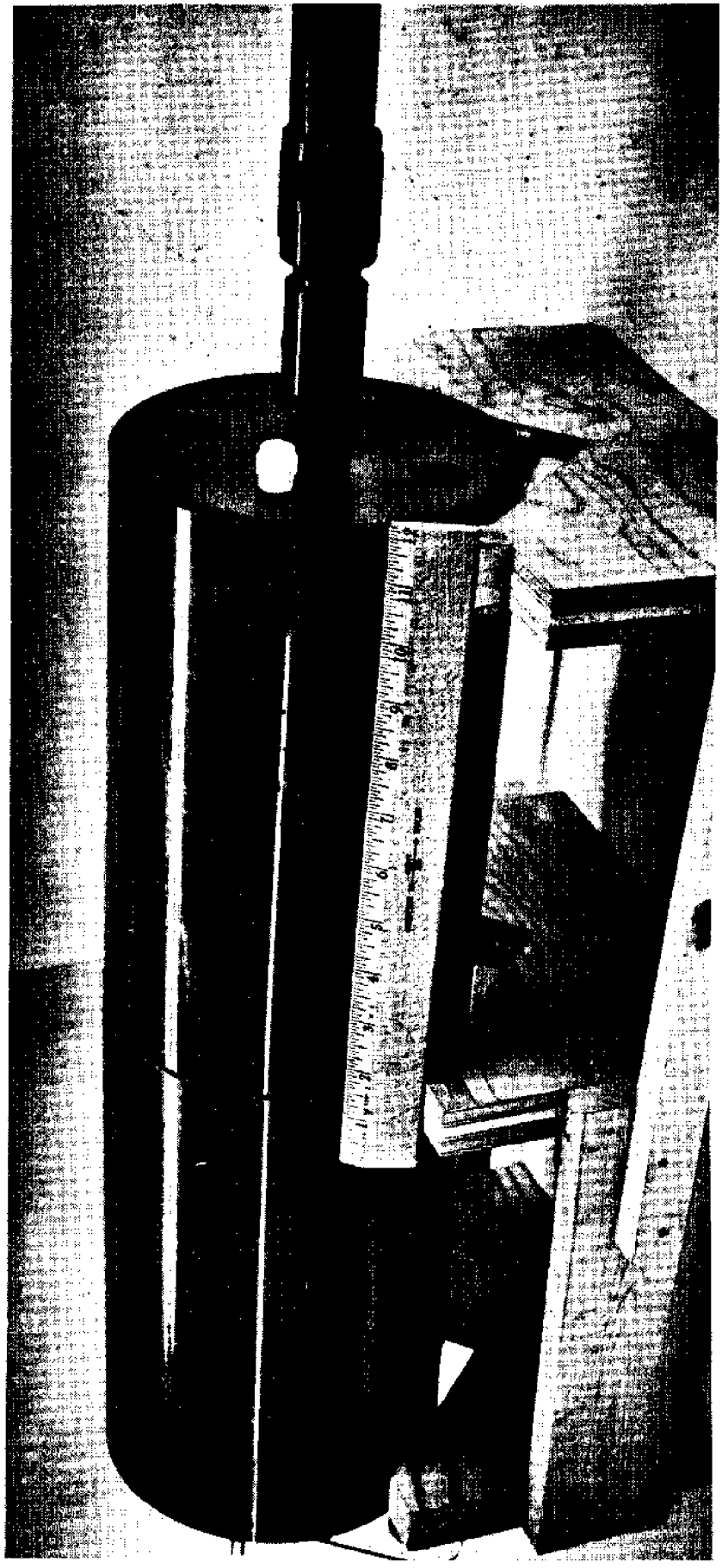

Figure 15. Instrument - Cover On.

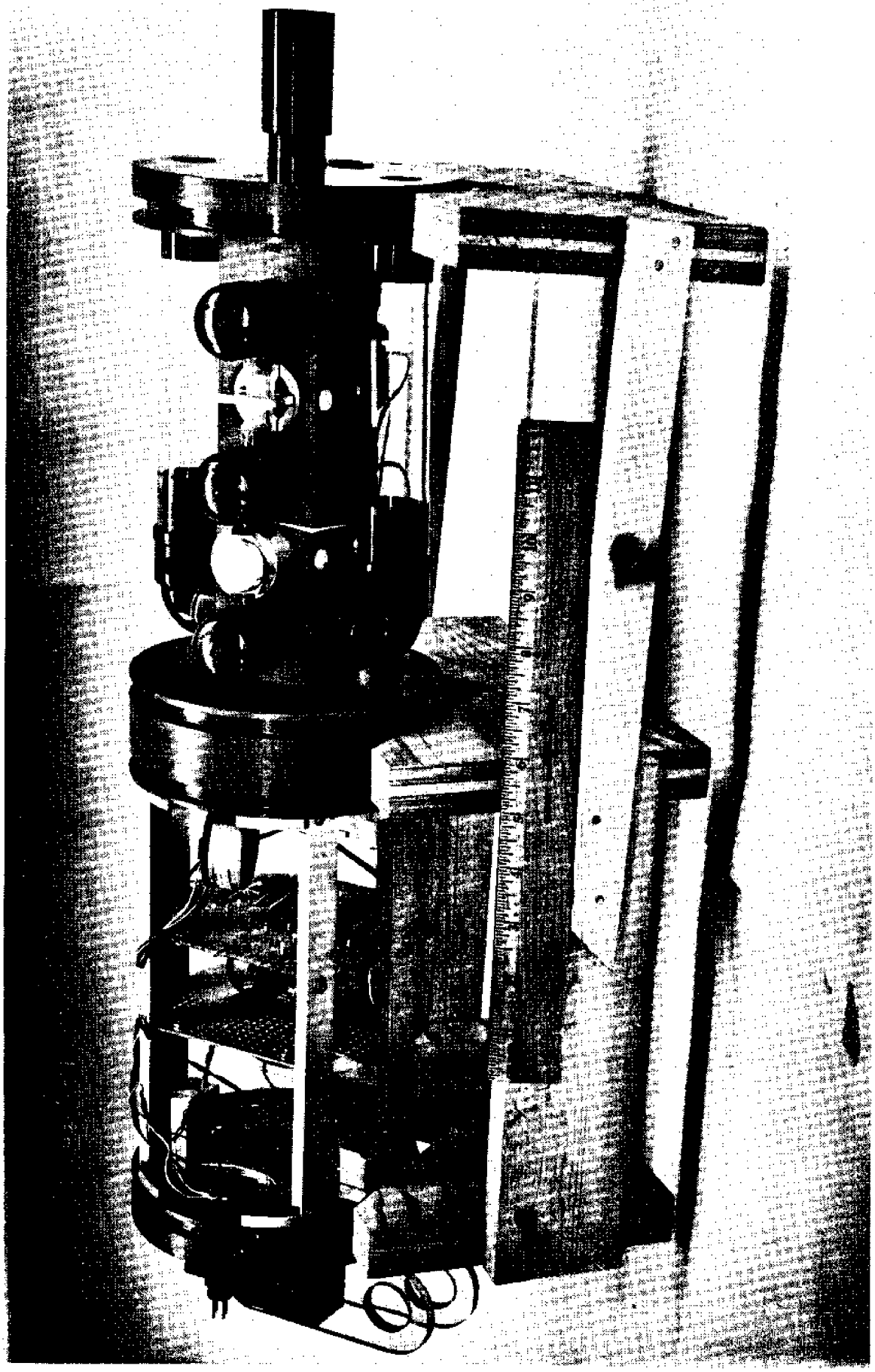

Figure 16. Instrument - Cover Off.

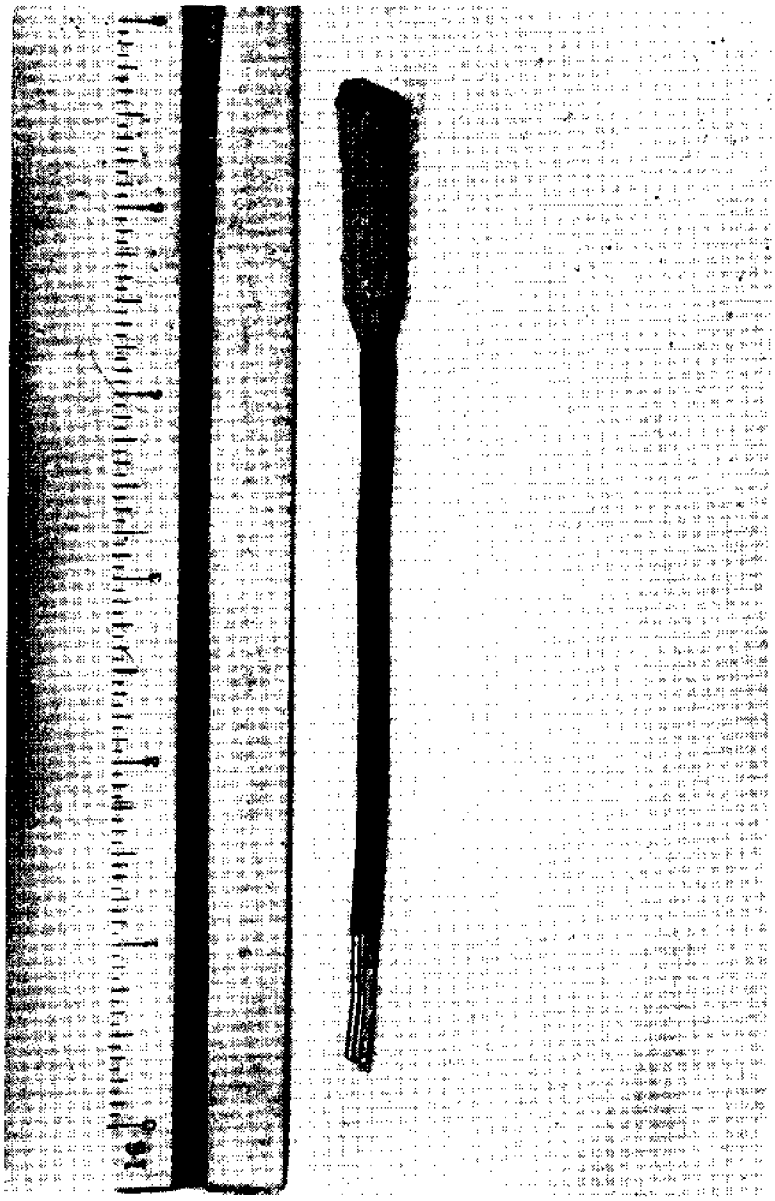

Figure 17. Silver Silver - Chloride Electrode.

salt bridge has low impedance through the sea water path along its length and very high impedance across the Tygon walls of the tube. Thus, as long as the impedance of the measuring circuit remains high, there is little voltage drop along the tube. There are no large thermal emf's in the salt bridge as there can be with the electrodes and the concentration emf's are less serious in the salt bridge also. Thus, the electrodes can be placed close together inside the housing of the GEK yet measure the potential in the water between widely separated points.

Figures 18 and 19 show the solenoids in the normal and energized positions (Point B). The valve between the electrodes is encased in metal (Point A) and cannot be seen, but it is closed in the normal position. The two solenoids are electrically connected in parallel, so that when one valve is open the other is closed and vice versa. The two pictures show how the solenoids pinch off greased 1/4-inch surgical rubber tubing to sever the sea water connection between the chambers in the manifold.

4) ELECTRONICS

Figure 20 shows the electronics section of the instrument. This section contains the pressure sensor, the amplifier circuit, and a battery pack to power the first stage of the amplifier circuit.

With an ocean current of 2 knots (approximately 100 cm/sec) and a salt bridge length of 20 meters, a typical signal between the electrodes would be 1 millivolt. The offset potential between the electrodes in the same sea water can sometimes be expected to be as great as 1 millivolt as well. Therefore, maximum signals at certain times can be expected to reach 2 millivolts. To maximize the signal sent up the cable yet avoid saturating the amplifiers at $\pm$10 volts, a voltage gain of 5000 is used in the amplifier of the GEK.

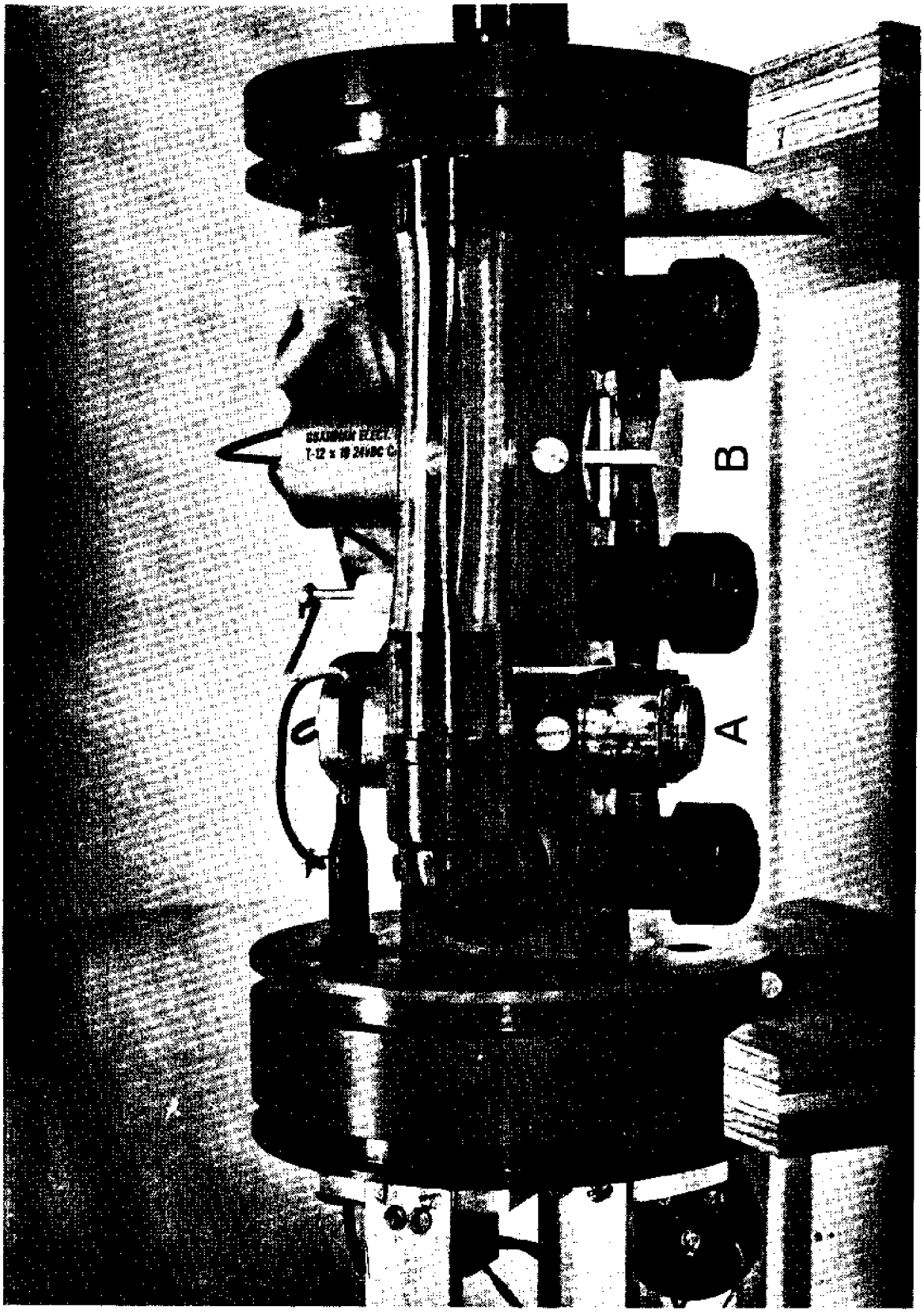

Figure 18. Electrode Section Solenoids De-energized.

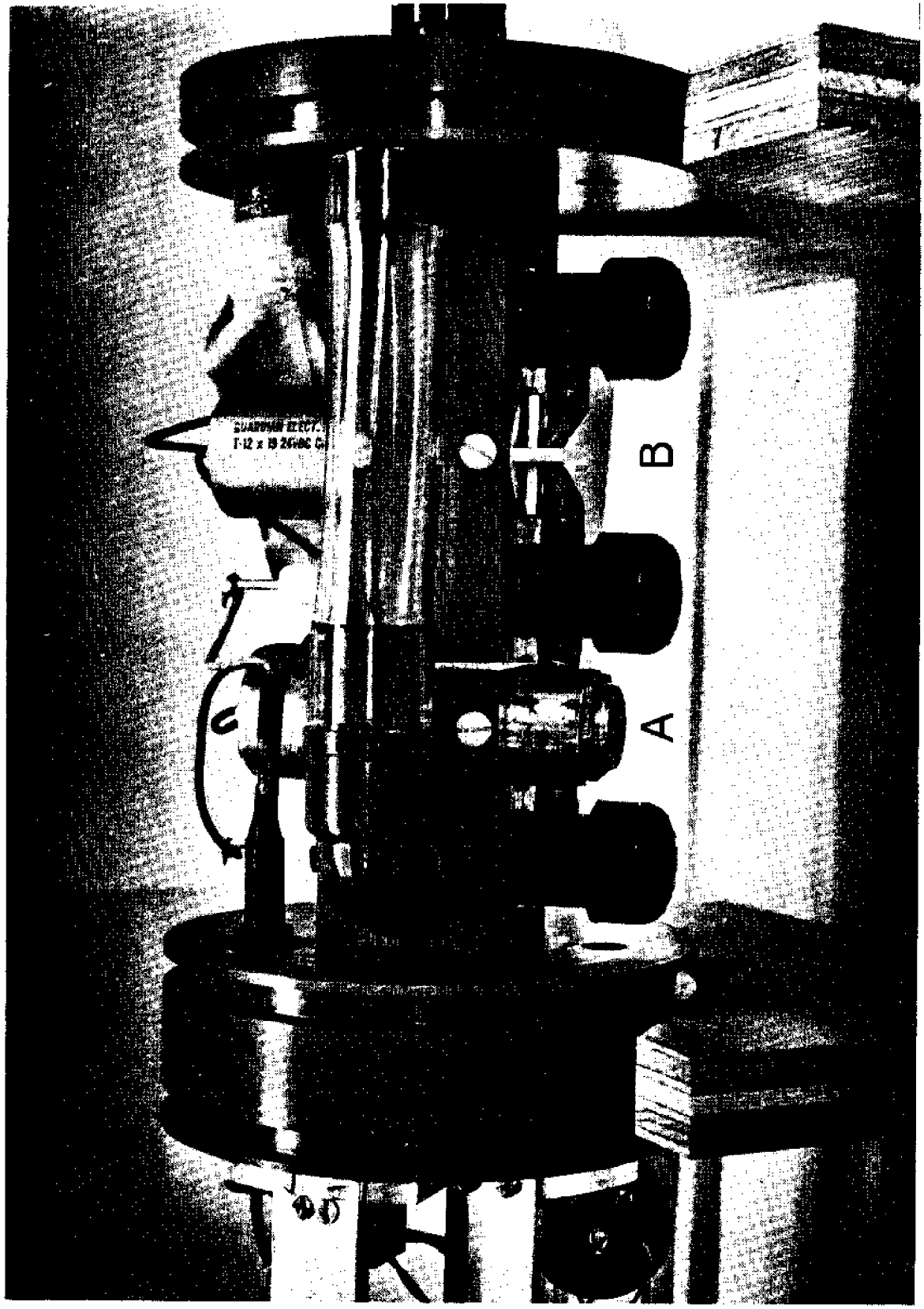

Figure 19. Electrode Section Solenoids Energized.

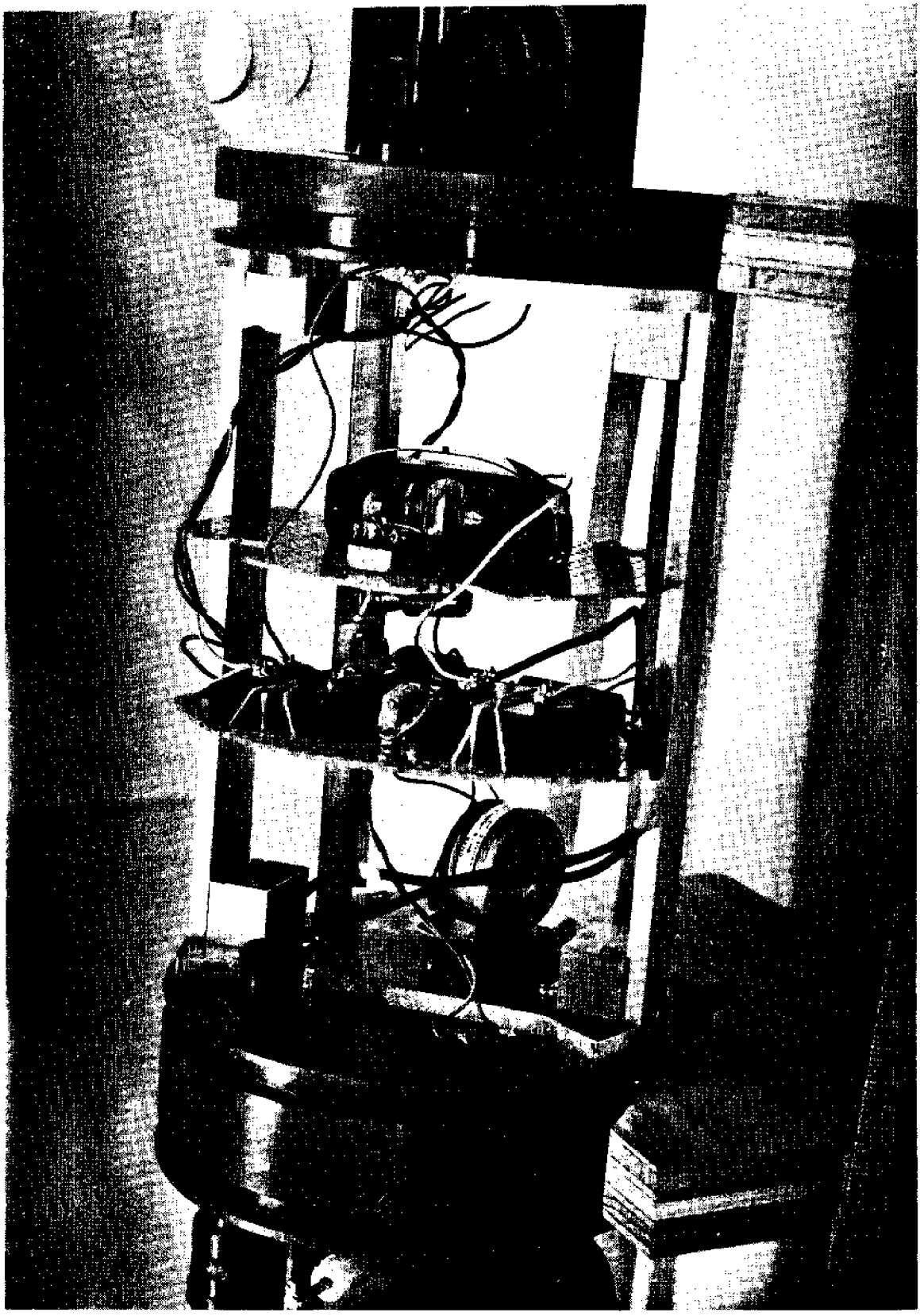

Figure 20. Electronics Section.

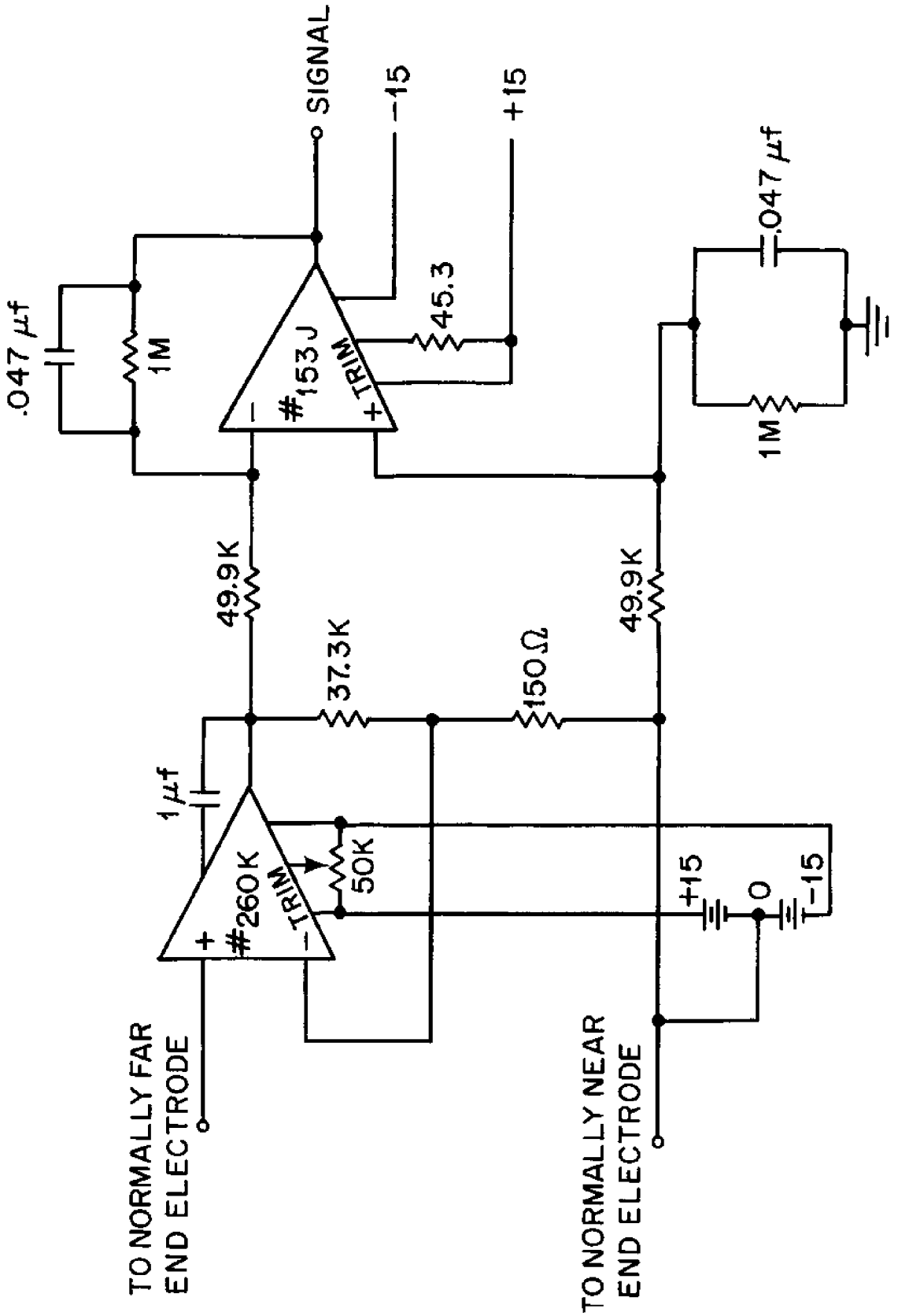

Figure 21. Electronic Amplifier Schematic.

Figure 21 shows a schematic diagram of the amplifier circuit. The amplifier consists of two operational amplifiers in series. The first stage has a gain of 250 and the second has a gain of 20 to give the total voltage gain of 5000. The first stage is a non-inverting amplifier with the high impedance input connected to the electrode which is normally in communication with the long salt bridge. A model 260K operational amplifier is used in the first stage. It has an extremely low temperature drift, 0.1 microvolts/°C, and a very large input impedance, 10^9 ohms. This high input impedance prevents loading of the electrode. The second stage uses a model 153J operational amplifier as a differential input amplifier. The operation of the amplifier circuit in the normal and switched modes is shown in Appendix 1. The three capacitors in the circuit control the frequency response of the amplifier. The capacitor values are chosen such that the high frequency roll off is 12 db/octave with the 6 db down point being at 3 Hz.

The connections between the electronics and the electrode section of the instrument are shown in Figure 22. The solenoids are connected in parallel at a pair of Mecca connectors (Point A). The electrode circuit is completed through an Electro-Oceanic connector which has coaxial beryllium copper contacts (Point B). This connector is used because of its small thermally generated offset voltage.

5) PRESSURE SENSOR

A bourdon tube pressure sensor with potentiometer readout is used in the instrument to monitor the depth of the housing. The inside of the bourdon tube is exposed to the oil pressure in the electrode section. Since sea water is not permitted to come in contact with the solenoids or solder connections, the entire electrode section (except for the electrode chamber itself) is filled with a light, non-conducting oil. In order to

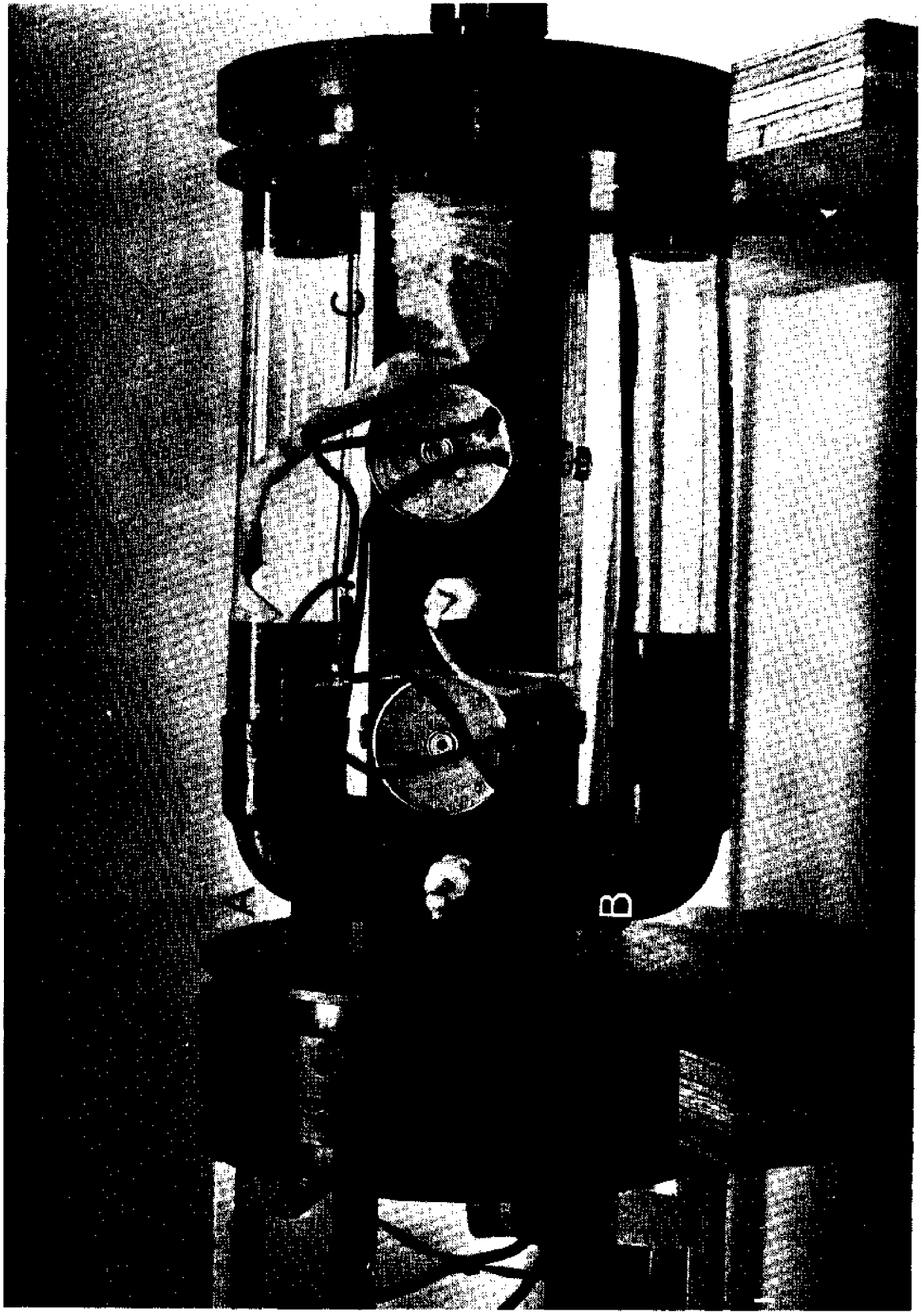

Figure 22. Electrode Section

equalize the pressure between the oil in the electrode section and the external sea water, a small compliant plastic bag open to the sea water is placed in the electrode section (Figure 22, Point C). As the water pressure increases, the bag expands and transmits the pressure increase directly to the oil.

Figure 23 shows an end view of the GEK. Point A is the tube which forms the long salt bridge. Points B and C are the openings of the short salt bridge. It is desirable to have the ends of both salt bridges lie on a line parallel to the ship's track to avoid cutting across the horizontal component of the earth's magnetic field.

This is in effect achieved by splitting the short salt bridge so it has two openings, one on either side of the long salt bridge. Point D is the opening to the compliant bag. Point E shows the plug for the oil filling hole.

6) MISCELLANEOUS EQUIPMENT

Several parts of the instrument and its support equipment deserve comment. Among these are the towing cable, the instrument case, and the salt bridge.

Galvanic currents from the ship or parts of the GEK or towing cable cannot be distinguished from currents of motional emf origin simply by switching electrodes. So an essential precaution for this instrument is the reduction of galvanic currents near the GEK to a negligible level. The instrument itself has no metal parts in contact with the sea (except of course the electrodes). A non-metallic electromechanical cable is used and 800 feet can be streamed to place the GEK far from the ship's field.

The underwater electrical connection between the GEK and the cable is made with 2 four pin plastic Glenair connectors shown in Figure 24. The pin type thru hull receptacles on the GEK are joined with the socket

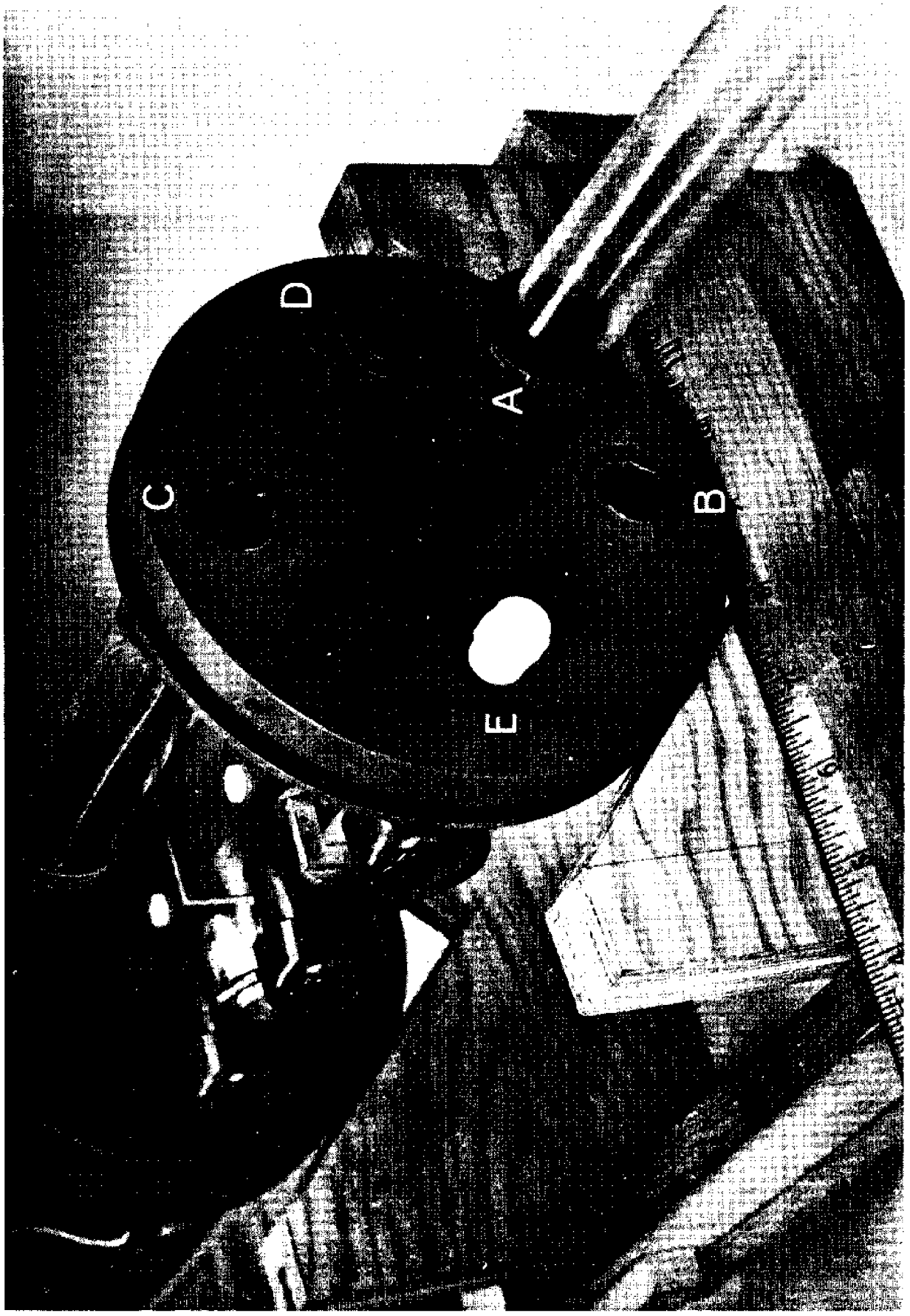

Figure 23. End view of Instrument.

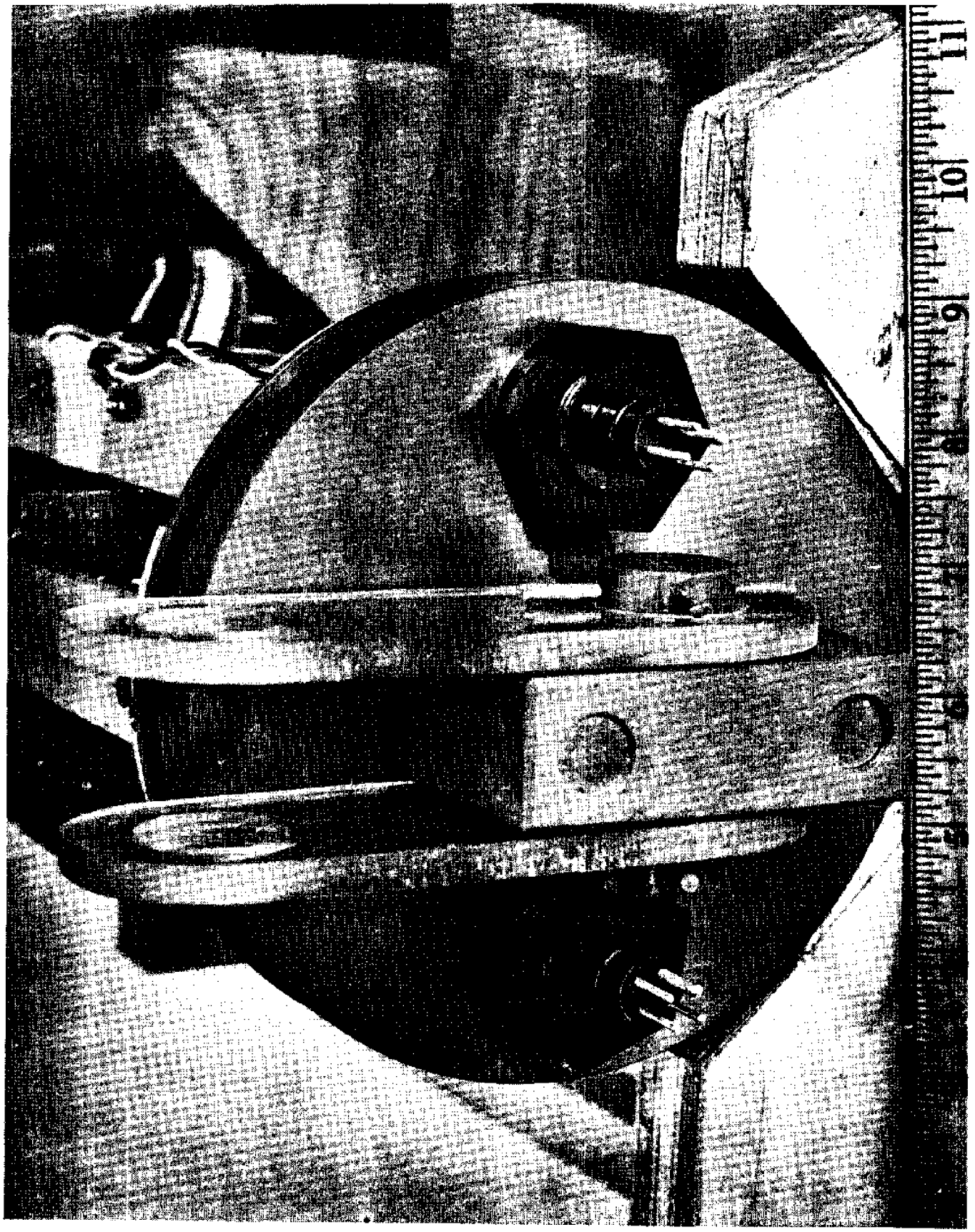

Figure 24. Front End of Instrument.

Figure 25. Female Connectors and Eye Splice.

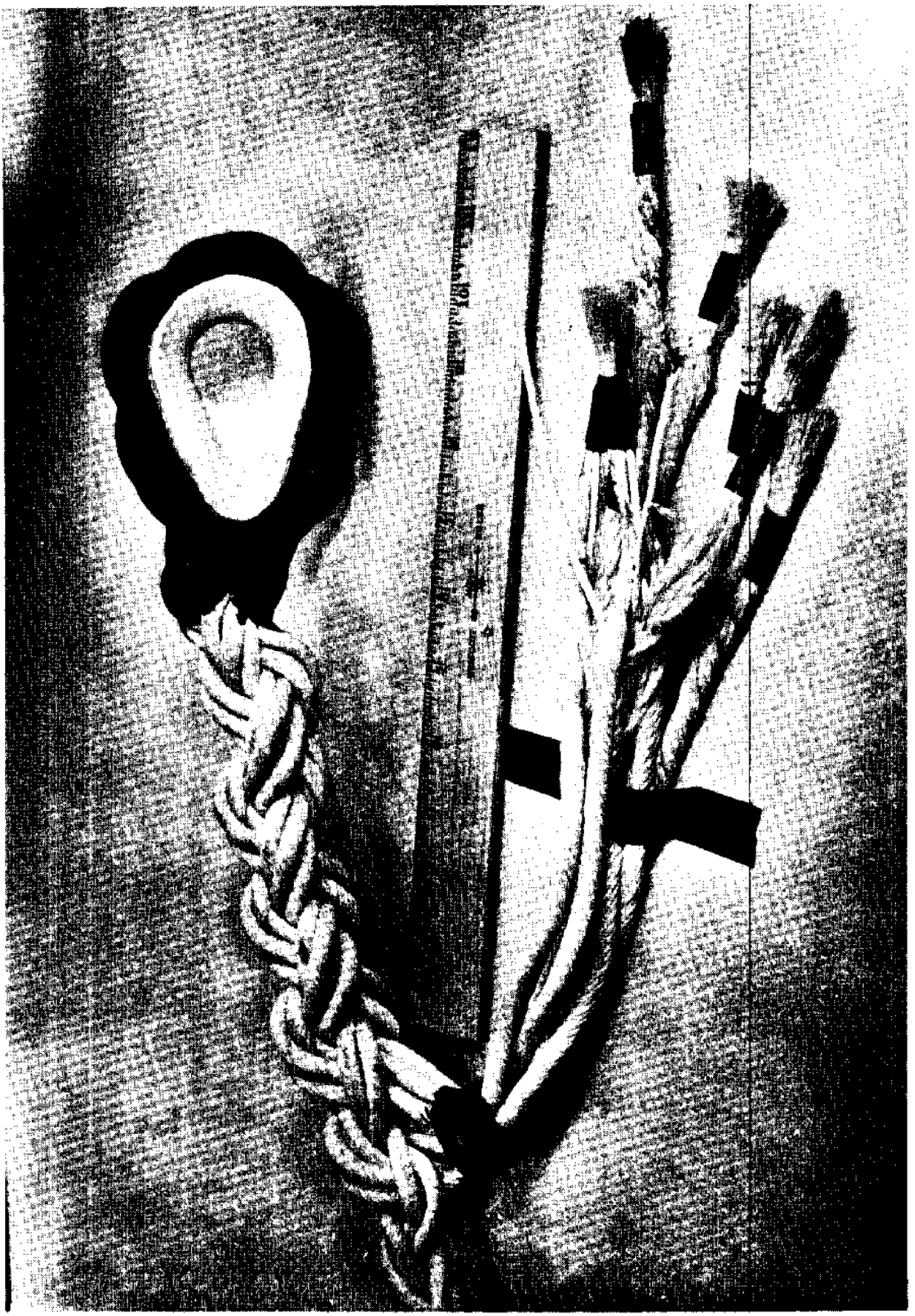

Figure 26. Eight Conductor Cable.

type cable plugs which are spliced to the eight conductors in the cable illustrated in Figure 25. The GEK is attached to the cable with the eye splice shown and a PVC bolt. The 7/8" diameter cable, which is plaited polypropylene, is shown in Figure 26 with some of the plastic coated wires exposed. The eight conductor cable can be stretched 10% without damage to the electrical wires because of their unique construction. Each electrical wire contains a copper conductor spirally wrapped around a nylon core, all of which are covered with a plastic waterproof jacket. Thus, when the rope stretches, the copper conductor straightens slightly. The cable is very slightly heavier than sea water.

A hand operated winch for reeling the cable and the attached GEK in and out is pictured in Figure 27. The cable conductors are terminated at a bulkhead connector through the winch flange. Once the cable is let out to the desired towing length, the winch is braked, and a shipboard eight conductor cable is plugged into the waterproof electrical connector on the winch (Figure 27, Point A). This cable connects to the recorder and power supplies.

The external housing for the GEK consists of two tubular PVC covers which slip over the electrode and electronics sections. The center bulkhead of the GEK has a slightly larger diameter than the ends so the radial O-ring seals need be engaged only for the last inch of assembly. The tubes do not carry any axial load so it is sufficient to position them with plastic screws. The axial load is carried by internal members. These tubular covers are shown in Figure 28.

One inch inside diameter Tygon tubing is used in the arms of the salt bridge. The tubing attaches to the end of the GEK with a PVC pipe coupling. Five and ten meter lengths are similarly joined together to make up to thirty meters of salt bridge. Modular lengths allow damaged pieces to be replaced easily and variable lengths to be deployed.

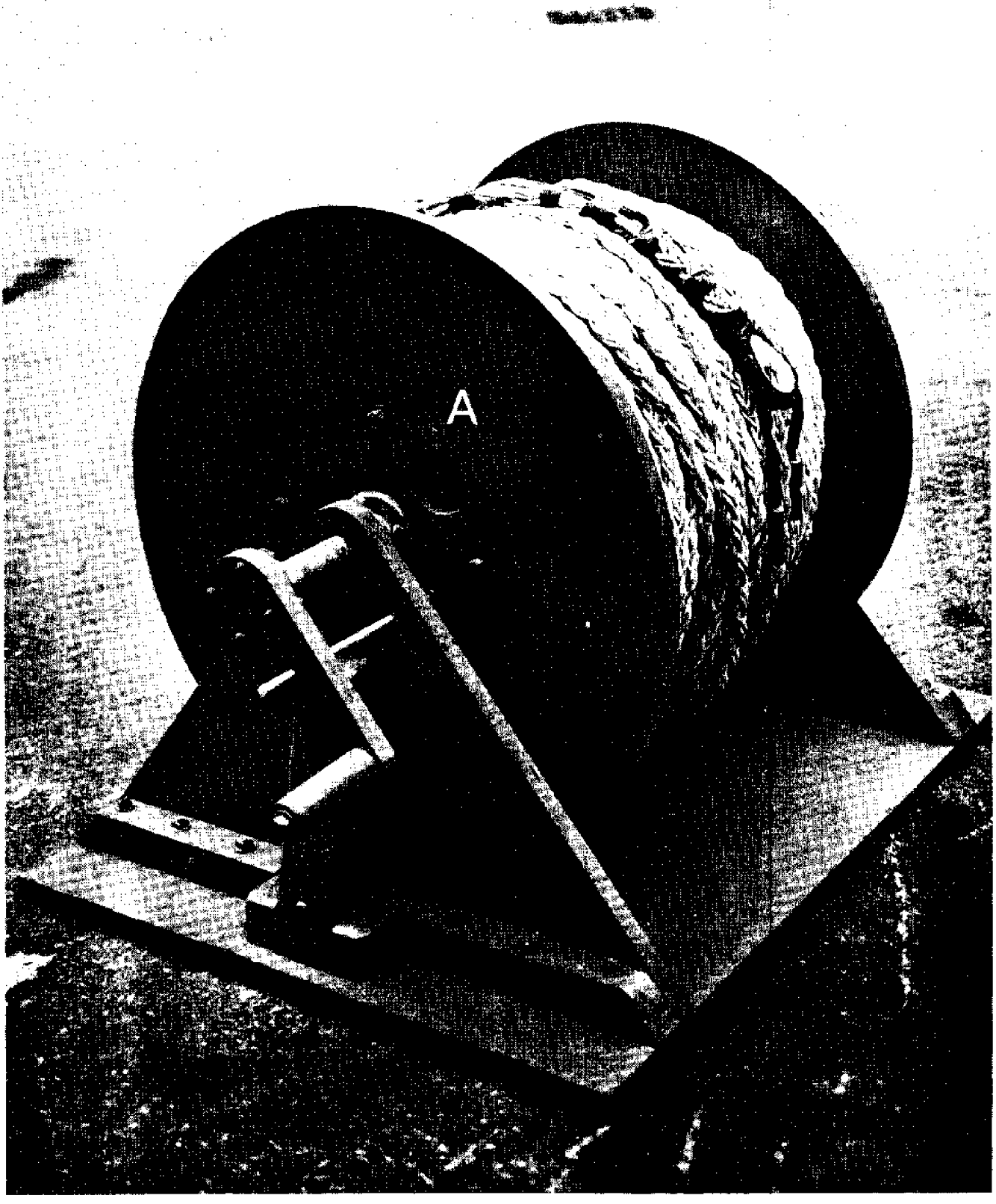

Figure 27. Winch

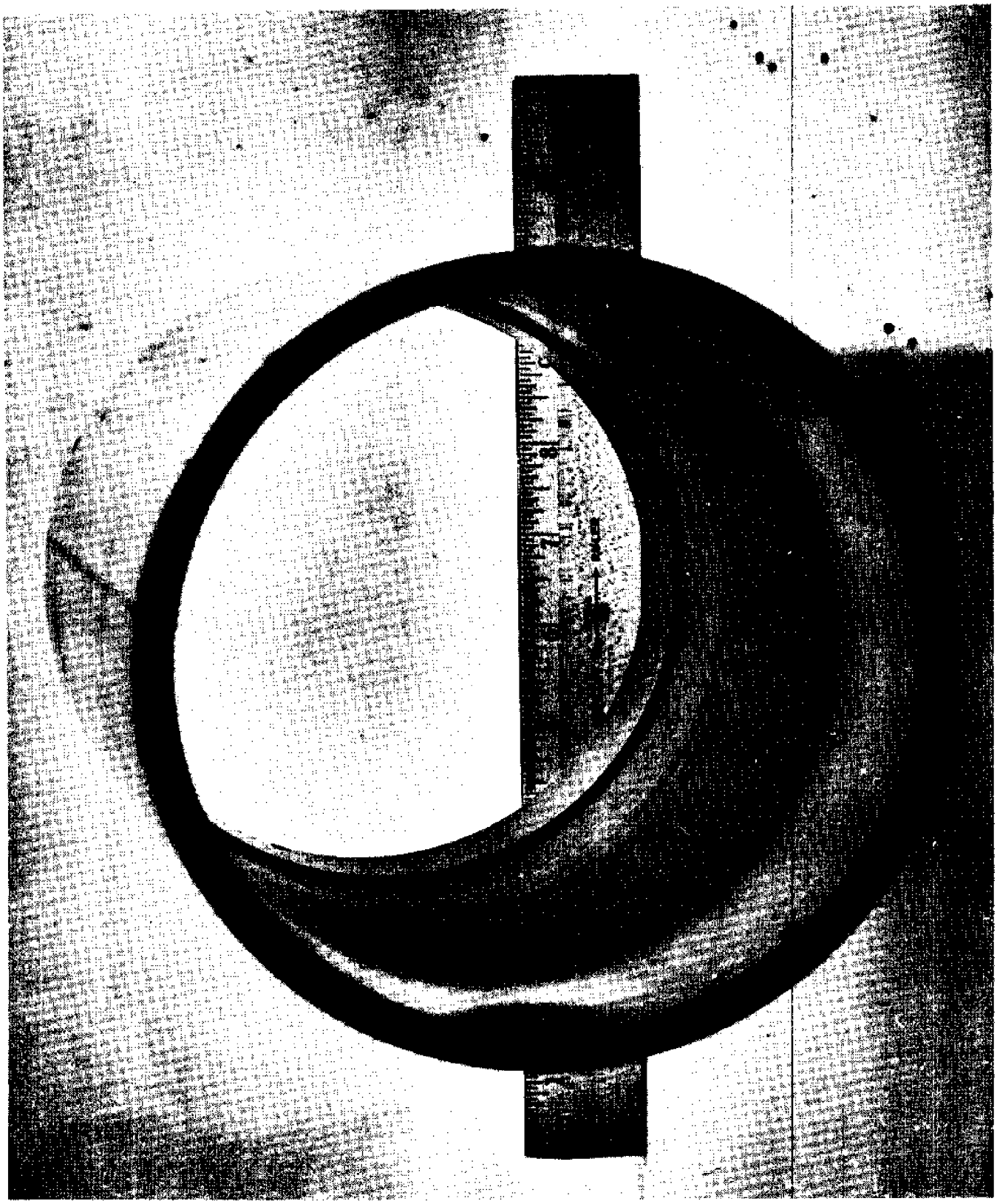

Figure 28. PVC Housing.

II. Instrument Problems and Their Solutions

During the course of the construction and testing of the surface GEK, many problems arose, several serious in nature. Although the electrode amplifier circuit was a straightforward and simple design, it proved to be quite obstinate in its refusal to operate properly. When wired on printed circuit board, the amplifier consistently oscillated at several hundred kilohertz and it was only by rewiring the circuit on perforated board with conventional leads that the circuit behaved. Then the circuit was wired into the GEK. But after intermittent malfunction on two field tests, it was discovered that oscillations reoccurred sometimes when the amplifier was powered through the cable. The problem was finally eliminated by putting 0.1 microfarad capacitors across the power input terminals of the operational amplifier of the second stage. This lowered the high frequency power source impedance.

A second type of problem which appeared in the first bottom deployment was the malfunction of one of the underwater Glenair electrical connectors. The connector was designed to provide a water tight seal but sea water seeped into the contact region. This caused an electrical short between several pins. The solution to this problem was to fill the connector with silicon grease before plugging it in. Sea water was thus prevented from reaching the pin connections.

A problem that was present on the first towing experiment and potentially on all towing experiments is the existence of air bubbles in the salt bridge. A large air bubble can cause an open circuit in one of the salt bridge arms. In the towed GEK, open circuits caused by air bubbles are most likely to occur in the rubber tubing near the valves. This is because the diameter of the salt bridge is smallest in this region. The existence of an open circuit causes the amplifier to saturate because offset currents at the input are

unshunted. The problem of air bubbles was greatly reduced by carefully filling the salt bridge with sea water and avoiding any air bubble entrapment during deployment in the water. Cotton plugs (Tampons) were then inserted in both arms of the salt bridge. The plugs allowed electrical conduction but little water transfer and air bubble entrapment in the salt bridge. In the bottom mounted configuration, air bubble problems were negligible because the increased pressure compressed the bubbles to insignificant size.

A serious problem which had to be recognized and eliminated in all GEK operations was the existence of ground loops. When an electrical path was present through the electrodes to ground and back to the electrodes through a sea water path, a significant electrical current passed through the electrodes and caused considerable drift in the electrode potential. Schematically, the existence of ground loops and how they were eliminated is shown in Figure 29. The actual ocean current is represented as a voltage source and resistor between points B and D. The sea water return path is shown by a resistor between points A and E. The Public Utility leakage voltage is shown as a voltage source between points A and E. It is seen that if the surface support power supplies and recorder are connected to Public Utility ground, an electrical path is completed and relatively large amounts of current will flow through the electrodes. However, if the surface support equipment has floating electrical grounds, then only circuit BCD is completed and a break is made between points E and D. Since the magnitude of the induced signal is on the order of tenths of millivolts and the input impedance of the measuring circuit is high, negligible current will flow through the electrodes. In the field experiments, ground loops were experienced when AC powered surface support equipment was used with the ground terminal

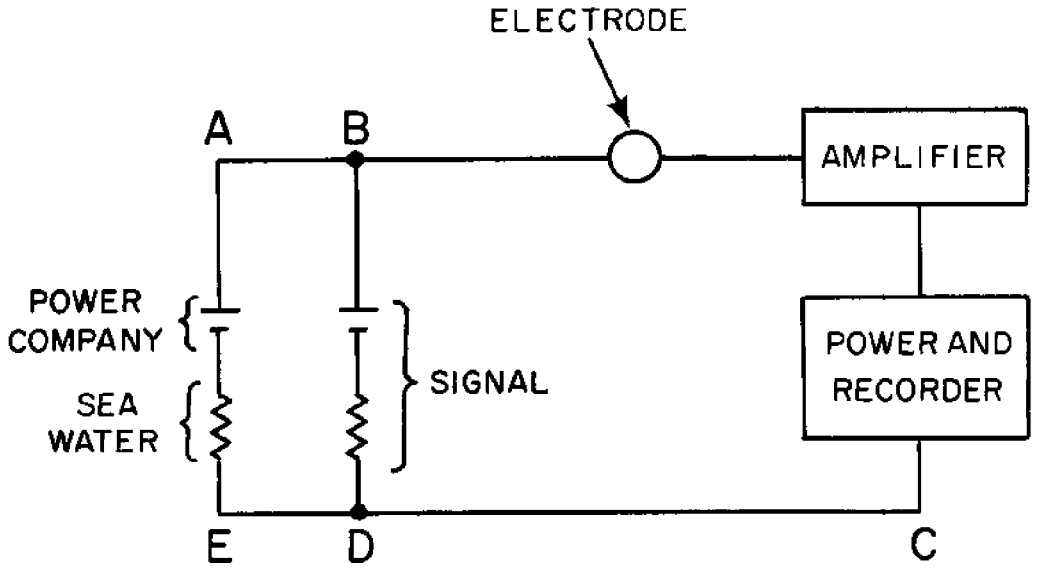

Figure 29. Ground Loops Schematic.

connected. Once the ground terminal was disconnected it was noted that the ground loops disappeared. In order to avoid all possibility of ground loops and to permit totally portable support, all power supplies were replaced by batteries and the recorder was converted to battery powered operation.

SECTION C

Laboratory and Field Tests of the Switched Electrode GEK, Both Towed on the Surface and Anchored on the Bottom.

I. Introduction

Laboratory tests on the towed GEK were conducted throughout its fabrication and field testing. The most important of these were the electrode drift tests. Field tests were conducted on the GEK during the last week in July and the first three weeks in August according to the following schedule:

ASTERIAS	27 July 1971
ASTERIAS	30 July 1971
Eel Pond	4 August 1971
Eel Pond	6 August 1971
Eel Pond	11 August 1971
ASTERIAS	13 August 1971
Gate of Canso	17-18 August 1971

II. Shakedown tests

1) TOWED TESTS

The first ASTERIAS cruise was conducted in Vineyard Sound. Although some data were obtained, this first cruise proved to be more valuable in checking out handling and shipboard procedures. As a result of this cruise, a vertical stand to facilitate filling the GEK with sea water was designed and fabricated (See Figure 30). It was also decided that the Tygon tubing should be filled ashore to ease the final assembly procedure on board ship.

The second ASTERIAS cruise was also conducted in Vineyard Sound. The towed GEK worked well during the preliminary shipboard tests, but later during

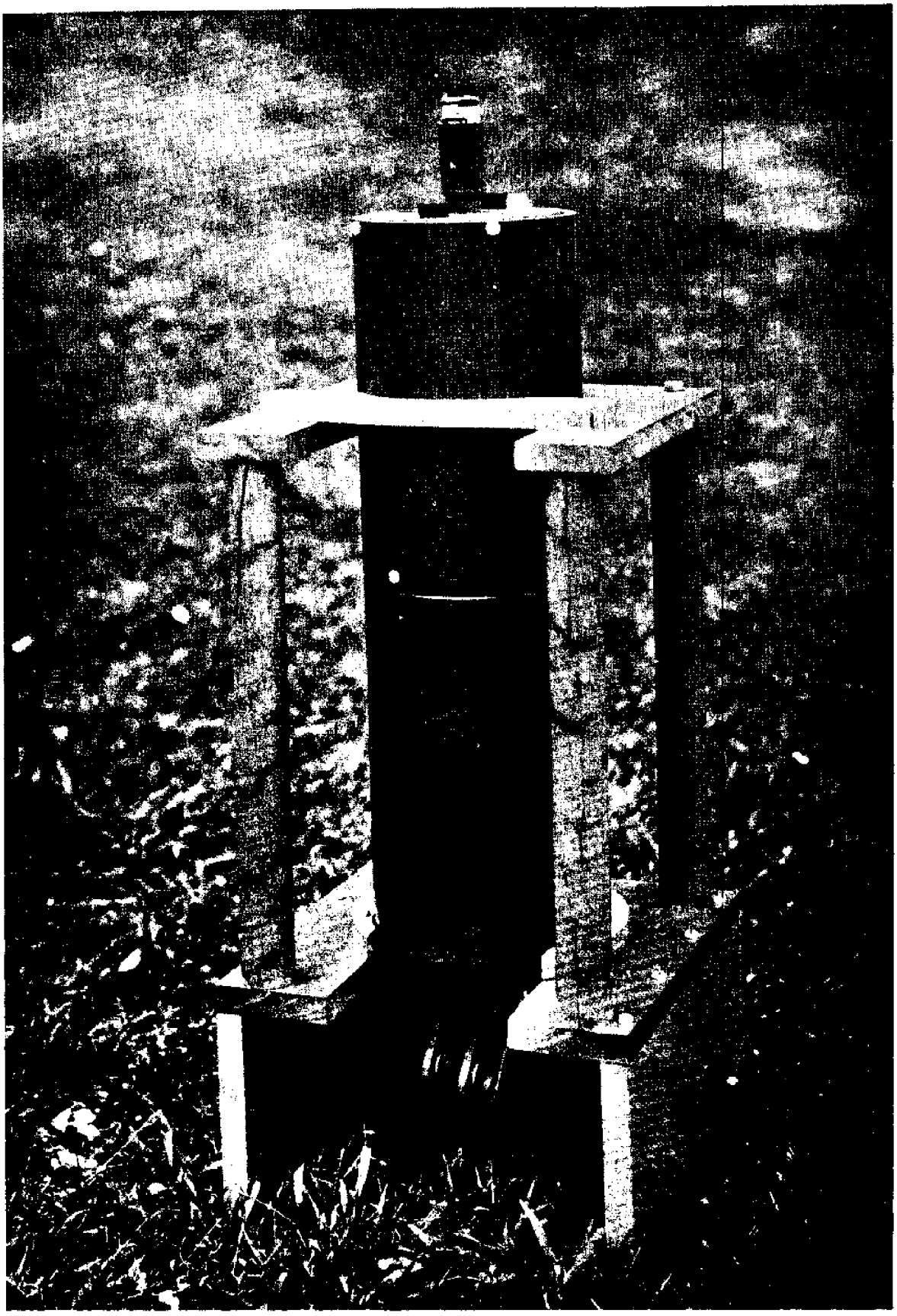

Figure 30. Vertical Stand.

a run across the Sound it developed problems; the amplifier saturated. At first it was thought that this was due to a bubble in the salt bridge, but laboratory tests conducted after the cruise showed that the cause of the problem was electronic oscillations associated with the cable impedance.

2) BOTTOM TESTS

The first bottom deployment was conducted in Eel Pond. The test site was approximately fifty feet from Eel Pond Bridge, near the Redfield parking lot. A fifteen meter length of tubing was laid across the channel on the bottom. Problems with rapid electrode drift and an imperfect Glenaire connector precluded the collection of worthwhile data. Laboratory tests were conducted to check on the electrode drift. The results of a 12-hour test showed that when the GEK was placed in a trough of salt water the electrode drift was only ±100 microvolts. The GEK was then placed in a bucket of salt water and the temperature was lowered to 9°C. As the temperature increased to 15°C, the potential between the electrodes increased 250 microvolts. In this test both electrodes were in contact with the same water. But neither of the results of the two tests could account for the large drift that was obtained in Eel Pond.

The second Eel Pond deployment had the same large rapid drift in the electrode offset. Tests held at the deployment site indicated a ground loop problem that was finally solved by eliminating AC power and operating from batteries.

III. Evaluation Tests

1) BOTTOM TESTS

The third Eel Pond bottom deployment yielded data which were free of the original ground loop and connector problems, but it is still not easy to explain them. The offset varied between 400 and 800 microvolts throughout the deployment. The signal was very high and fairly stable at 800

±160 microvolts above the offset. It appeared as if there were a constant field in the area of the GEK with an alternating component riding on top of this DC level. At first it was thought that this might be due to the presence of large power cables in the vicinity of the site, but if this had been true than the same effect should have been seen on the first two Eel Pond deployments. The data also differed from previously obtained data in that it was unnaturally noise free. The data was plotted to see whether the AC component corresponded to what one would expect from the previous data (DC component removed). These data showed sole correspondence to the natural seiche period of Eel Pond but the correlation was not very good.

2) TOWED TESTS

The third ASTERIAS cruise, using a 20 meter salt bridge, appeared free of all problems. The track of this cruise appears in chart 1, and the results are given in Figures 31 and 34. Course A-B runs from Tarpaulin Cove to Paul Point. The data indicate a west flow on one side of Middle Ground and an east flow on the other. This agrees with the predictions of Eldridge's 1971 Tidal Current Charts (White 1970). Course B-C runs from Paul Point to the cable area near Lake Tashmoo. Course C-D follows the cable to Nobska Point. From this record we can see that flow is now totally eastward, which is again in agreement with Eldridge. Course D-H contains a series of 90° turns: D to E and F to G, running approximately parallel to the current; and E-F and G-H, running across the current in opposite directions. The latter tracks should be opposite in polarity but of the same magnitude. Figure 34 shows the approximate agreement. The conversion of $(V-\overline{V}^{*}) \times B$ in microvolts, to current in knots, is given in Appendix 2 (100 microvolts is approximately .2 knots). Using this value in converting the data for course A-B, we obtain a maximum west flow of .4 knots and an east flow of .2 knots. This again agrees with Eldridge.

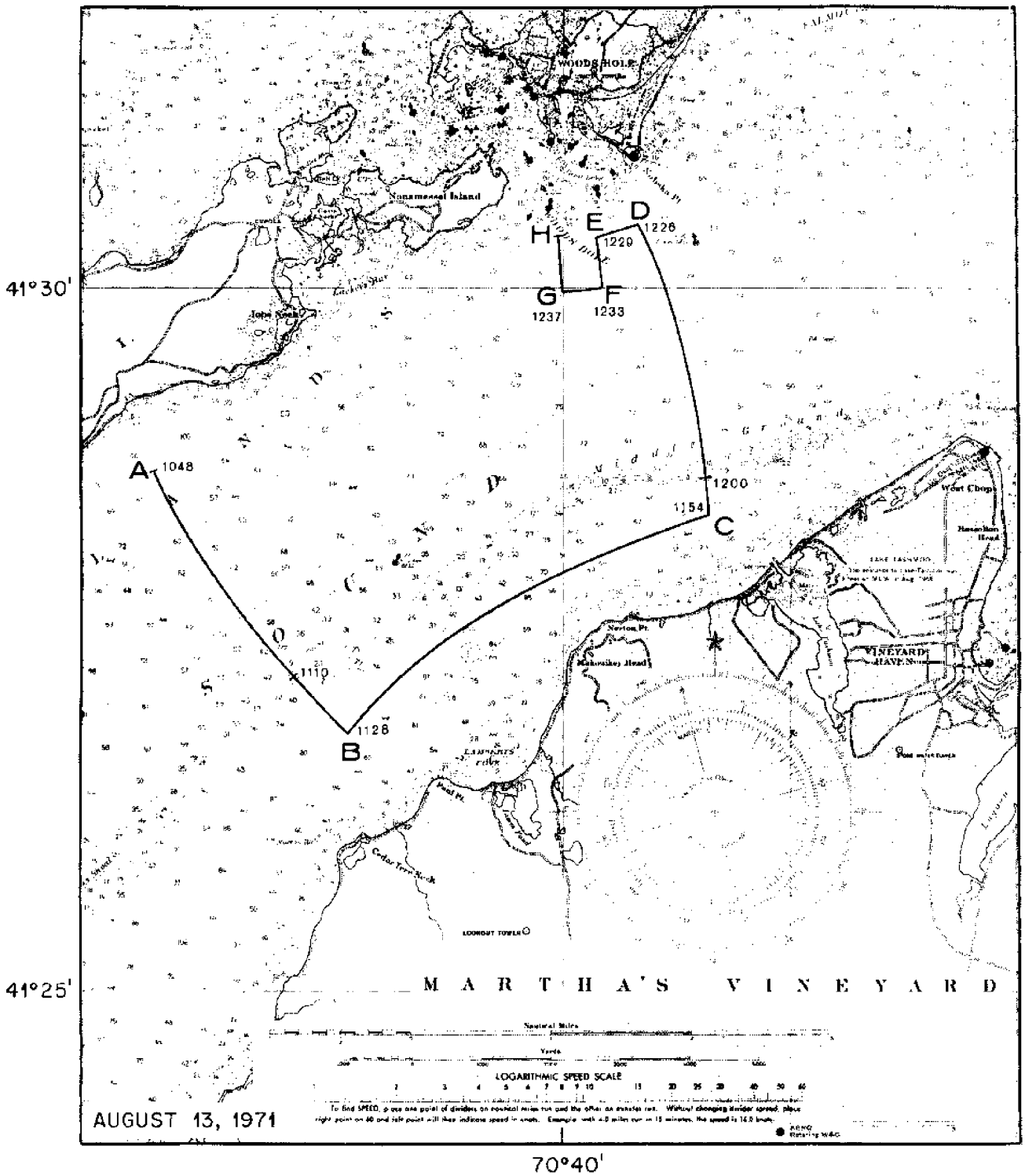

Chart I. Course of Asterias August 13, 1971.

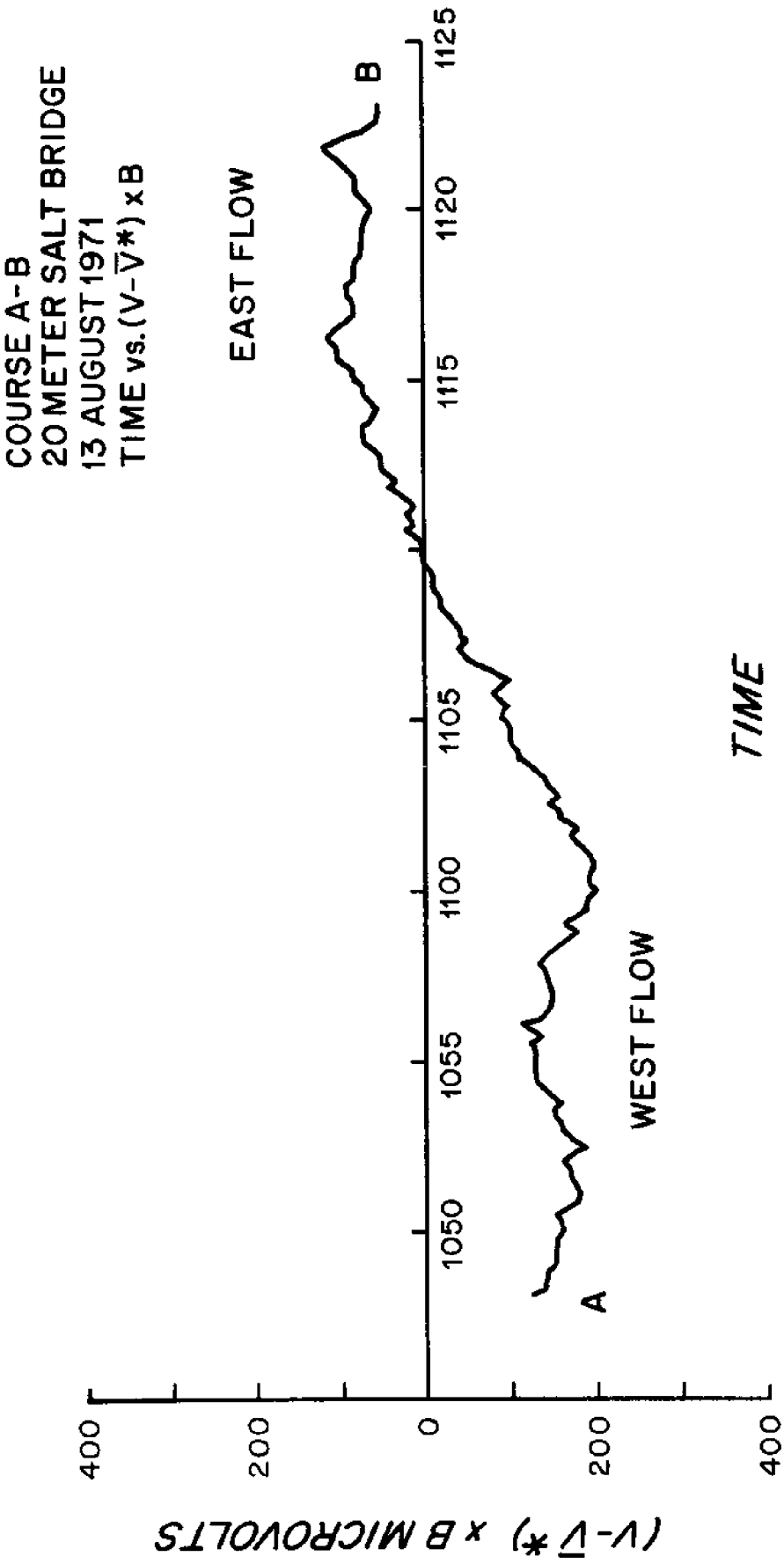

Figure 31. Course A-B August 13, 1971.

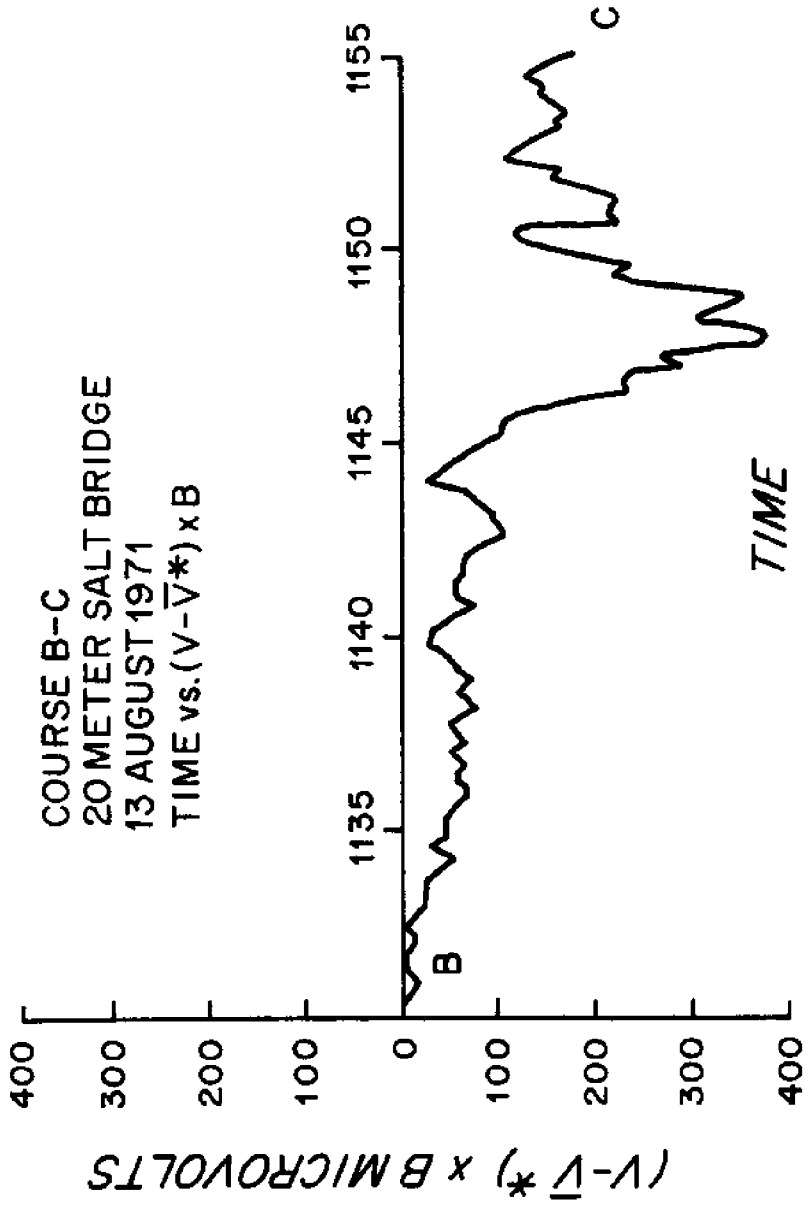

Figure 32. Course B-C August 13, 1971.

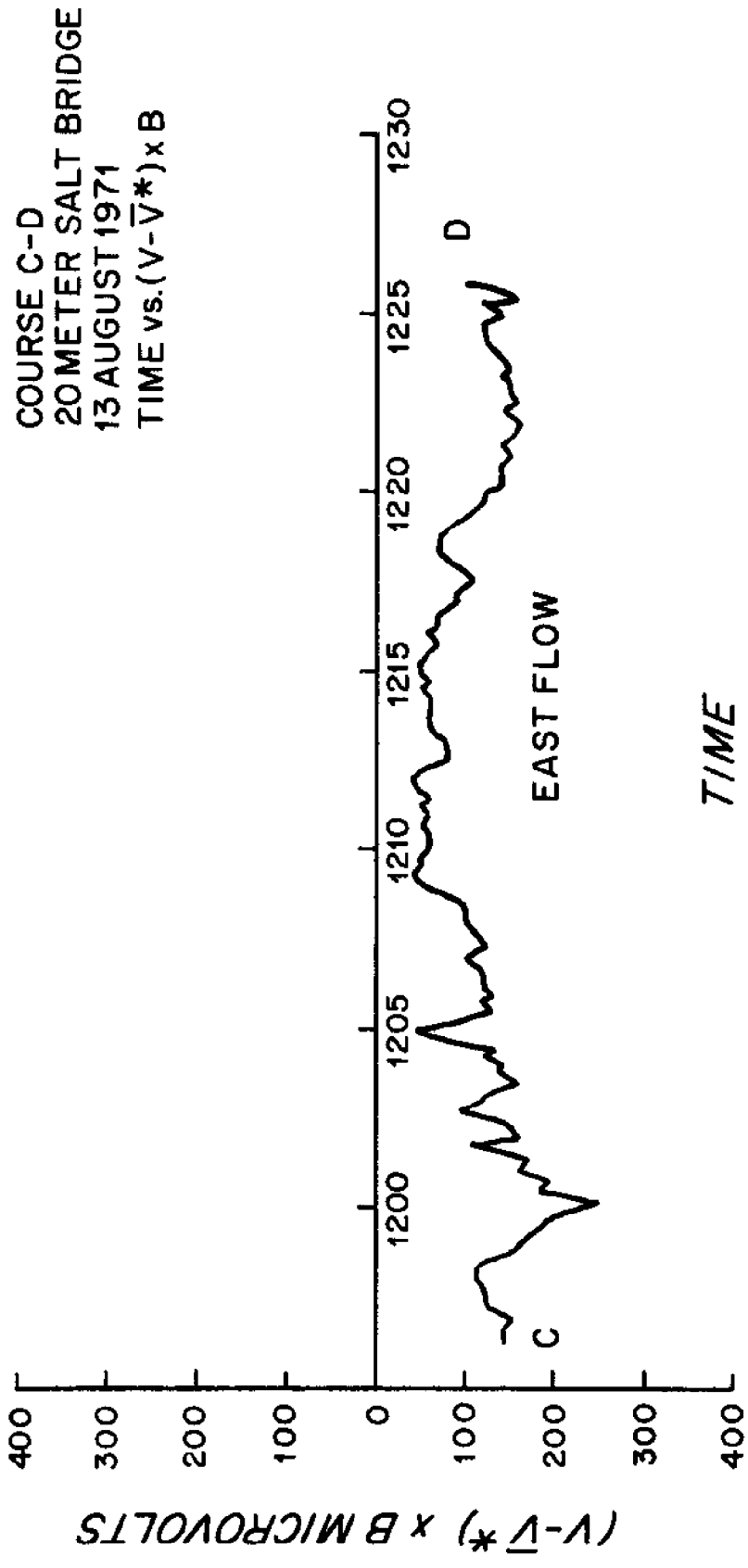

Figure 33. Course C-D August 13, 1971.

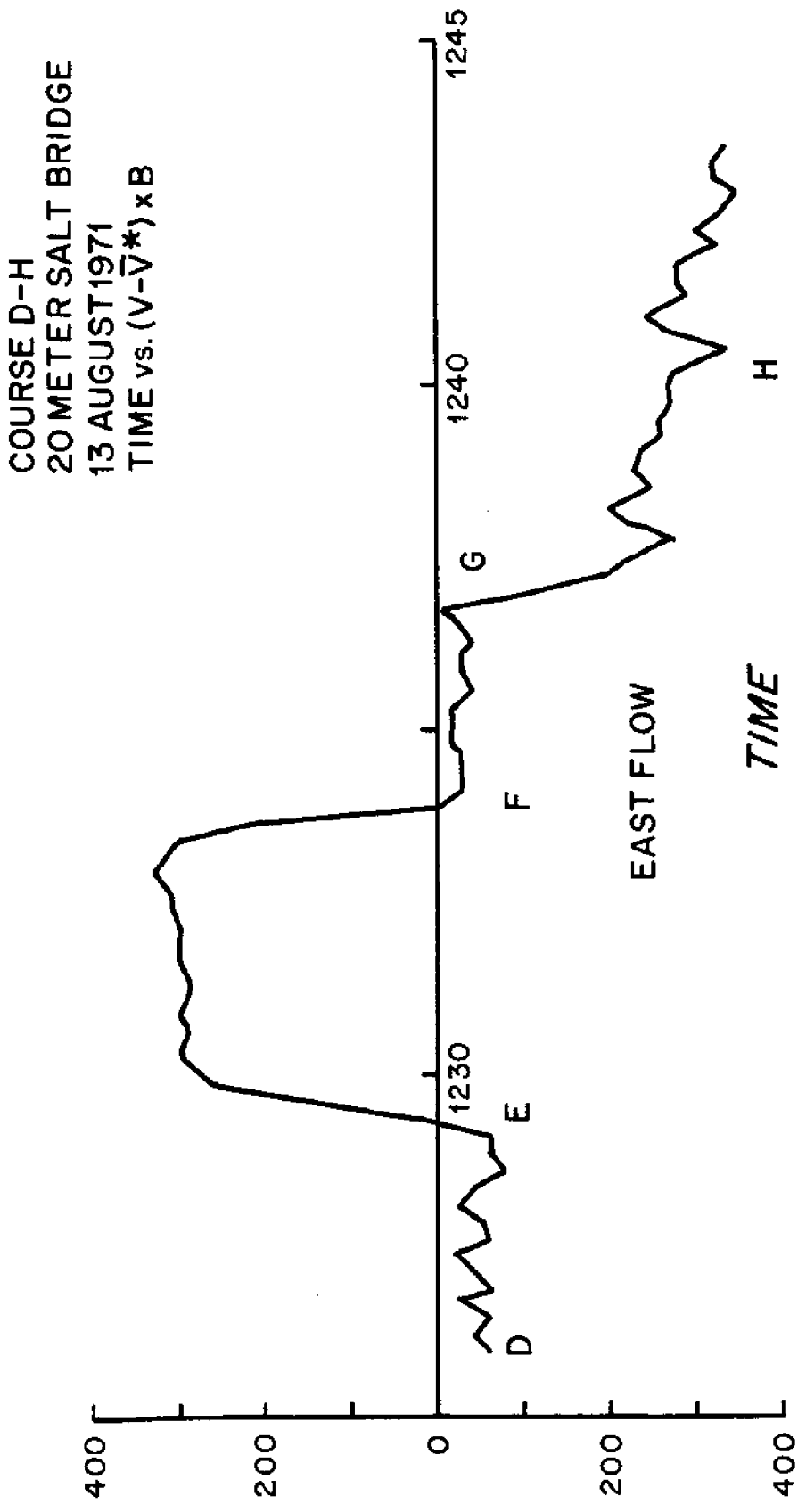

Figure 34. Course D-H August 13, 1971.

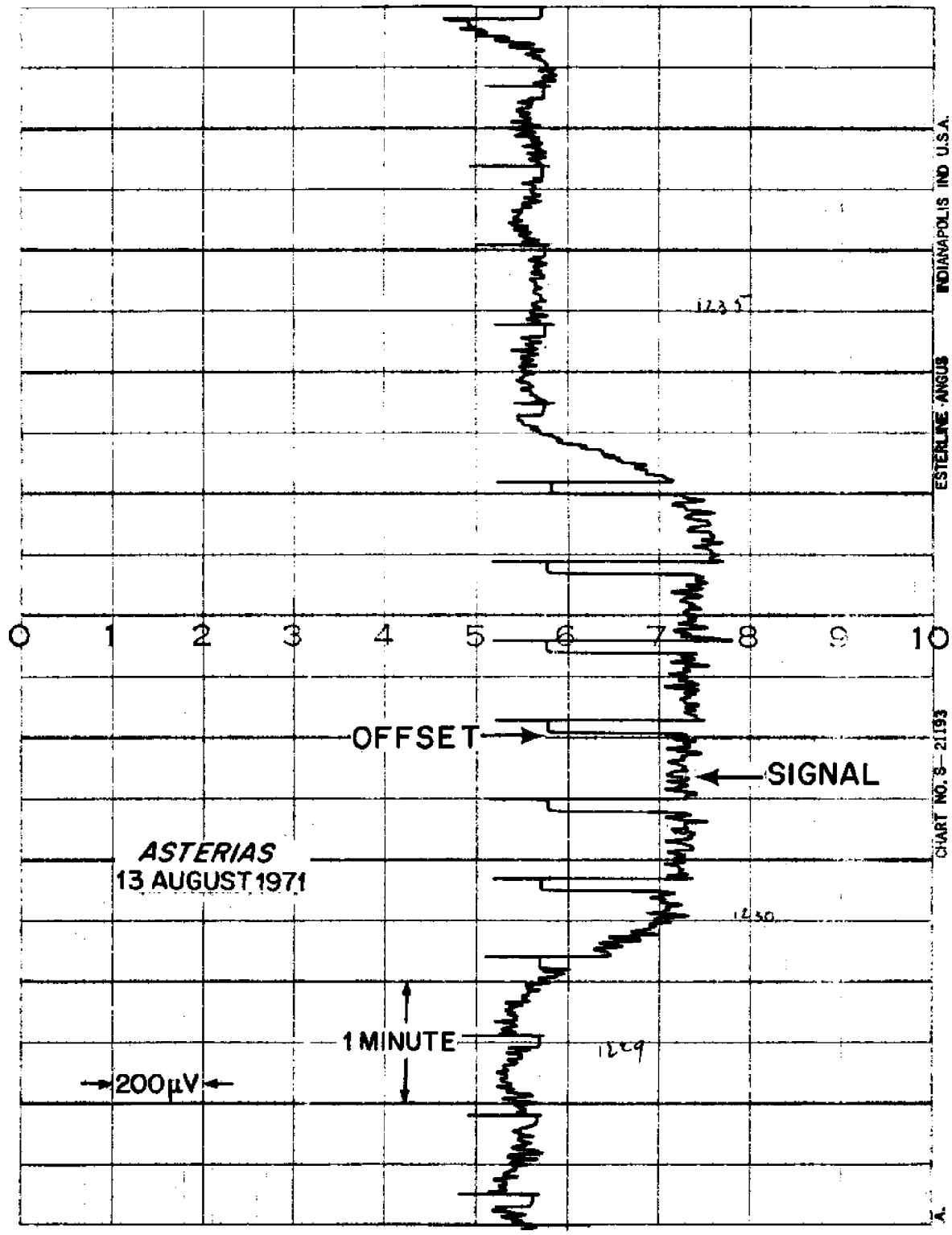

Figure 35. Typical Data-Asterias August 13, 1971.

Figure 35 shows typical raw data obtained from the third ASTERIAS run. The signal superimposed on top of the expected signal is noise, which can be filtered out. This noise decreased as the towing speed of the GEK decreased, as the length of the towing cable was increased, and as the sea state decreased.

IV. Deployment Test on Bottom at Gate of Canso

The last field test was conducted in the Gate of Canso (See Chart II). This test area was selected because of its lack of power cables, accessibility, high currents, and excellent fishing. The GEK was anchored on the bottom in 15 feet of water and a 30 meter salt bridge was stretched across the channel under the region of significant current flow. Data from this test are contained in Figures 36 to 40.

The incoming flow was more turbulent than the outgoing flow due to the geometry of the site. The incoming flow contained much upwelling and downwelling which might account for some of the variability of the signal. Figures 41 and 42 are samples of raw data that show the marked difference in character of the signal for the two flows.

The electrode offset potential drift was also plotted for the Gate of Canso deployment. The plot of this is shown in Figures 43 and 44. Initial deployment in the Gate of Canso resulted in a rapid offset potential decrease from 1000 microvolts to 450 microvolts in approximately one and one half hours. This was probably due to temperature effects caused by the new environment. For the next several hours there was a steady decrease in the offset potential to less than 200 microvolts until a recorder malfunction interrupted the measurement. Upon re-acquisition of the signal, the offset potential was 200 microvolts ±100 microvolts for the duration of the deployment.

In the Gate of Canso, the bottom conductivity affects the voltage observed across the current. The conversion of $\overline{V}^{*}$ x B, in microvolts, to current in knots, is given in Appendix 2 (100 microvolts is approximately

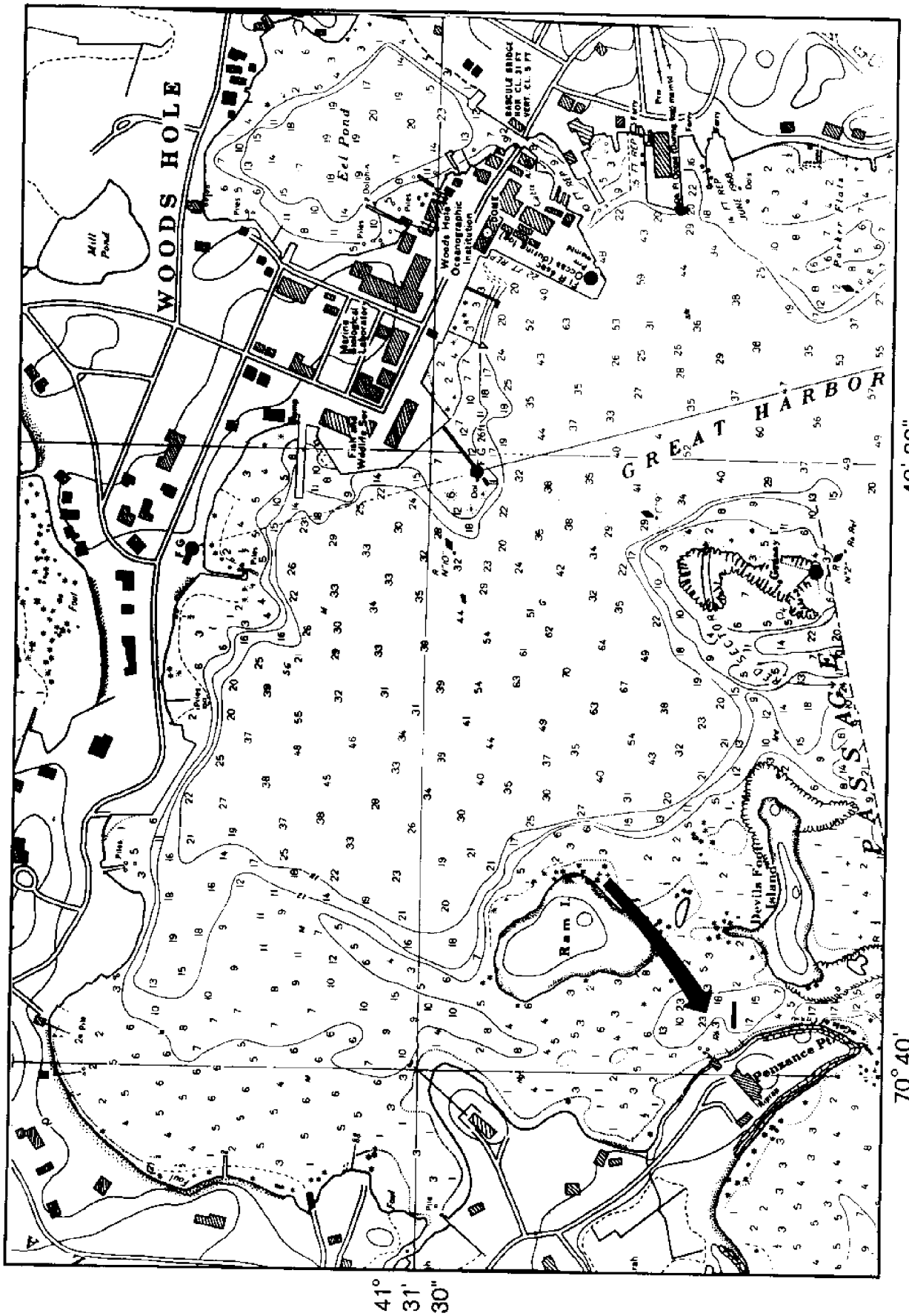

Chart 2. Gates of Canso August 17 & 18, 1971 Bottom Deployment.

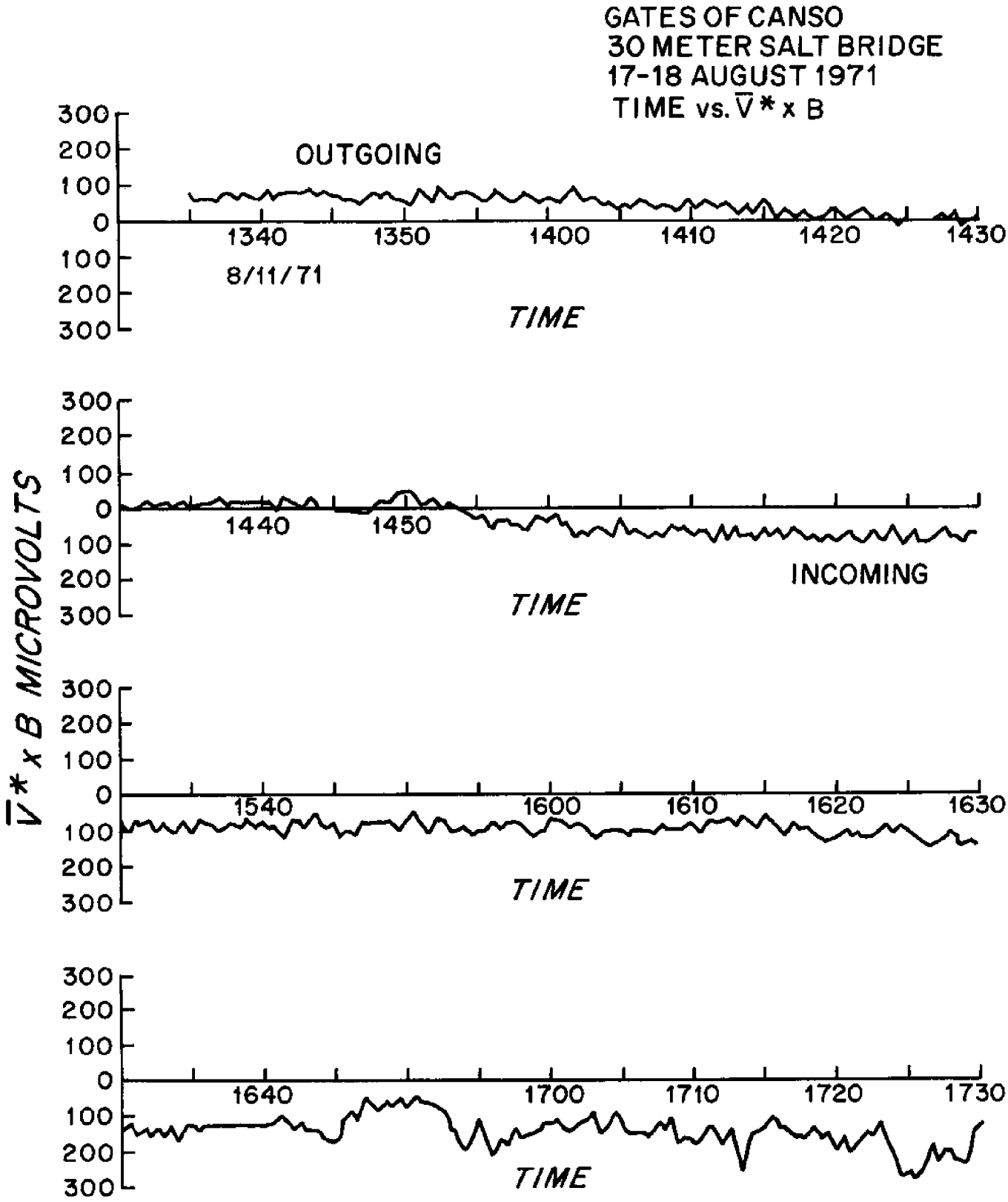

Figure 36. Gates of Canso 1330-1730.

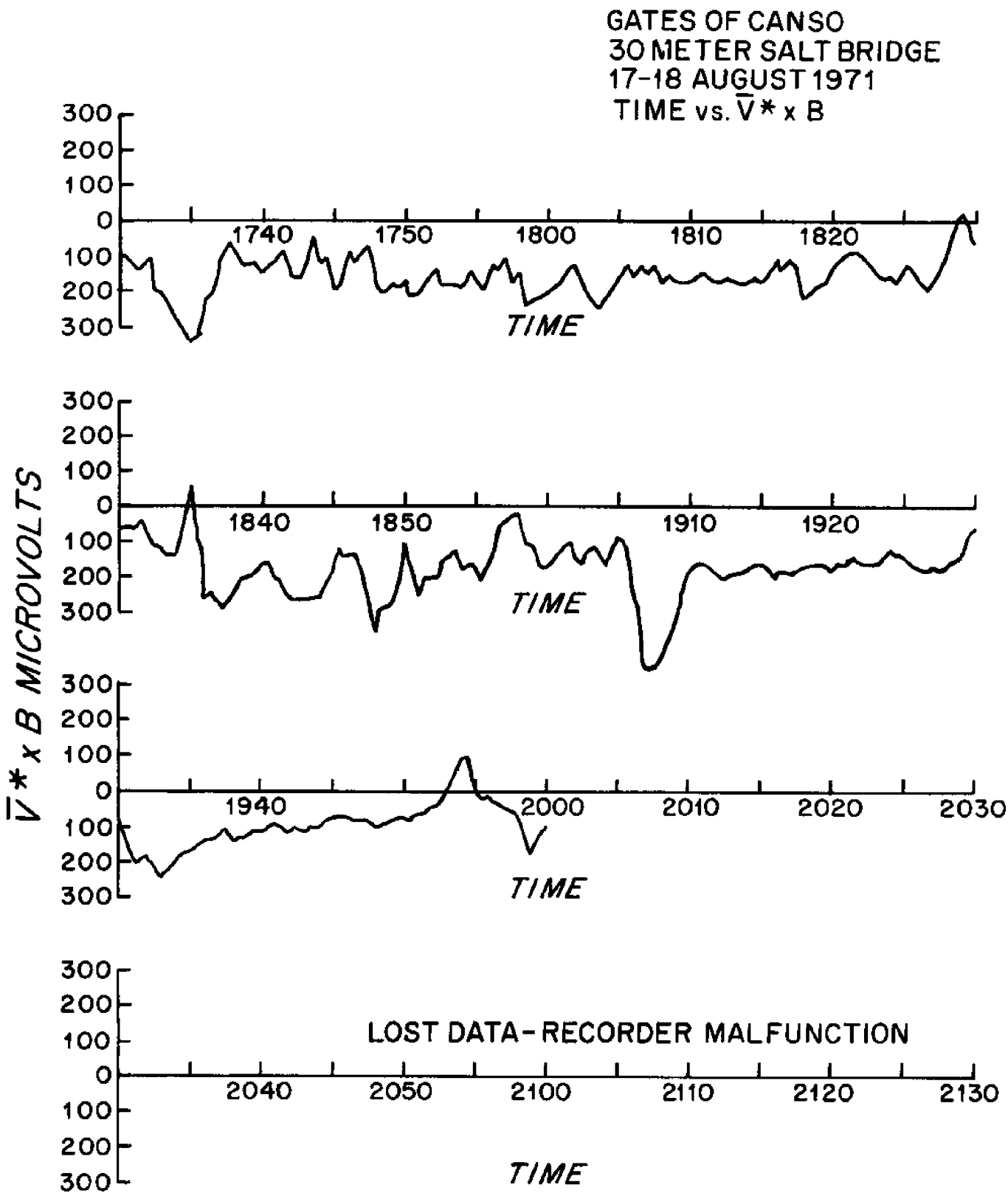

Figure 37 Gates of Canso 1730-2130.

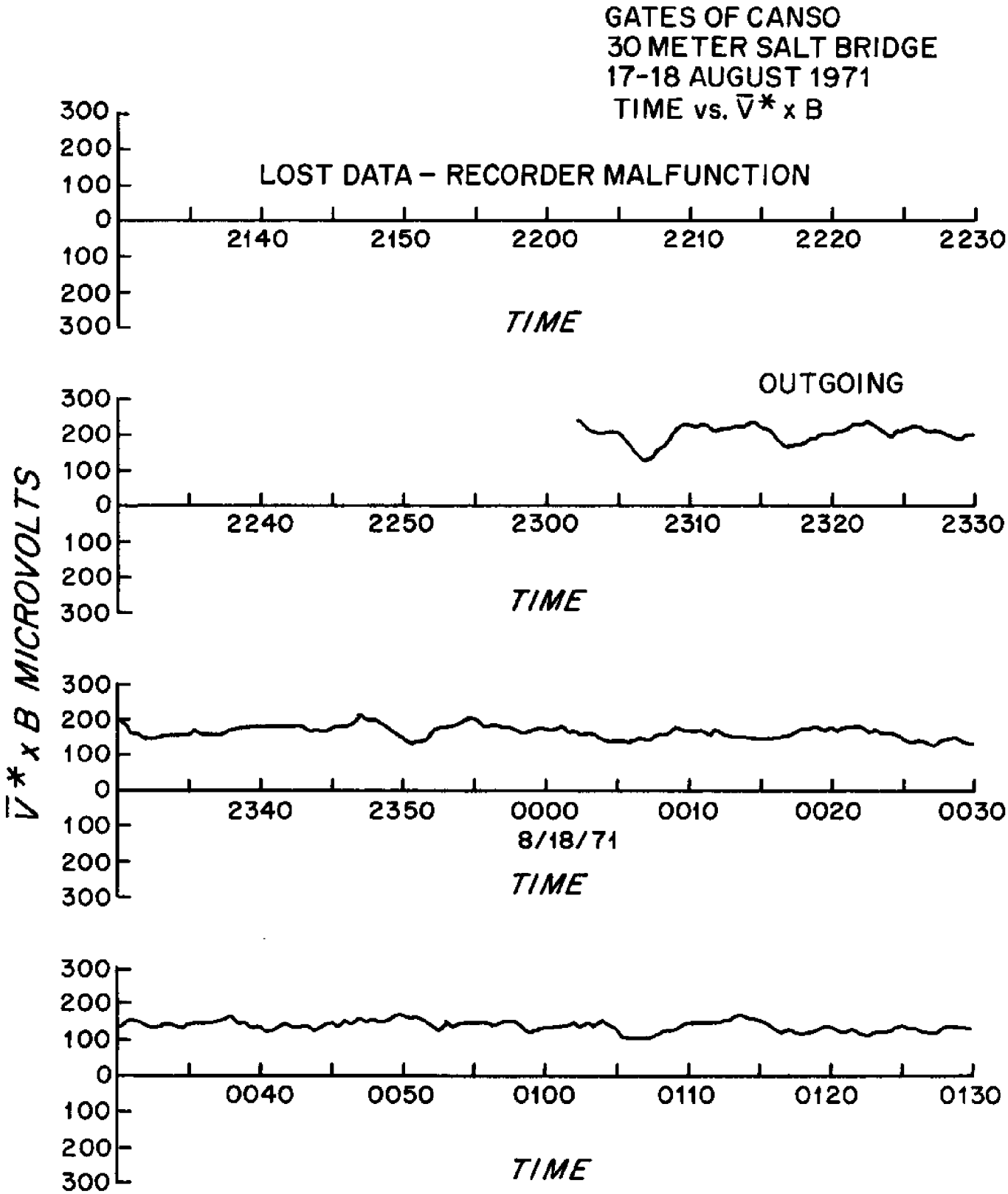

Figure 38. Gates of Canso 2130-0130.

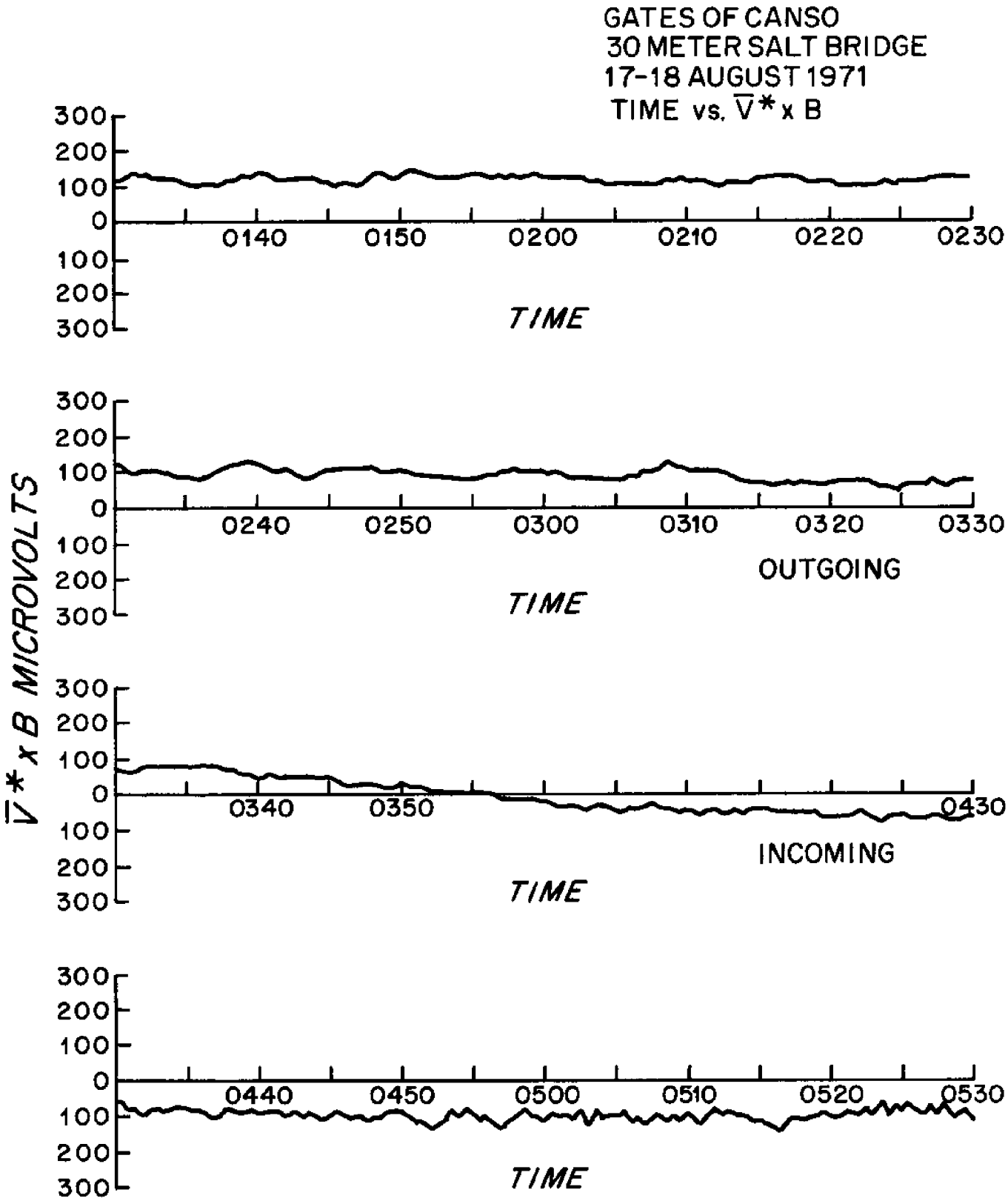

Figure 39. Gates of Canso 0130-0530.

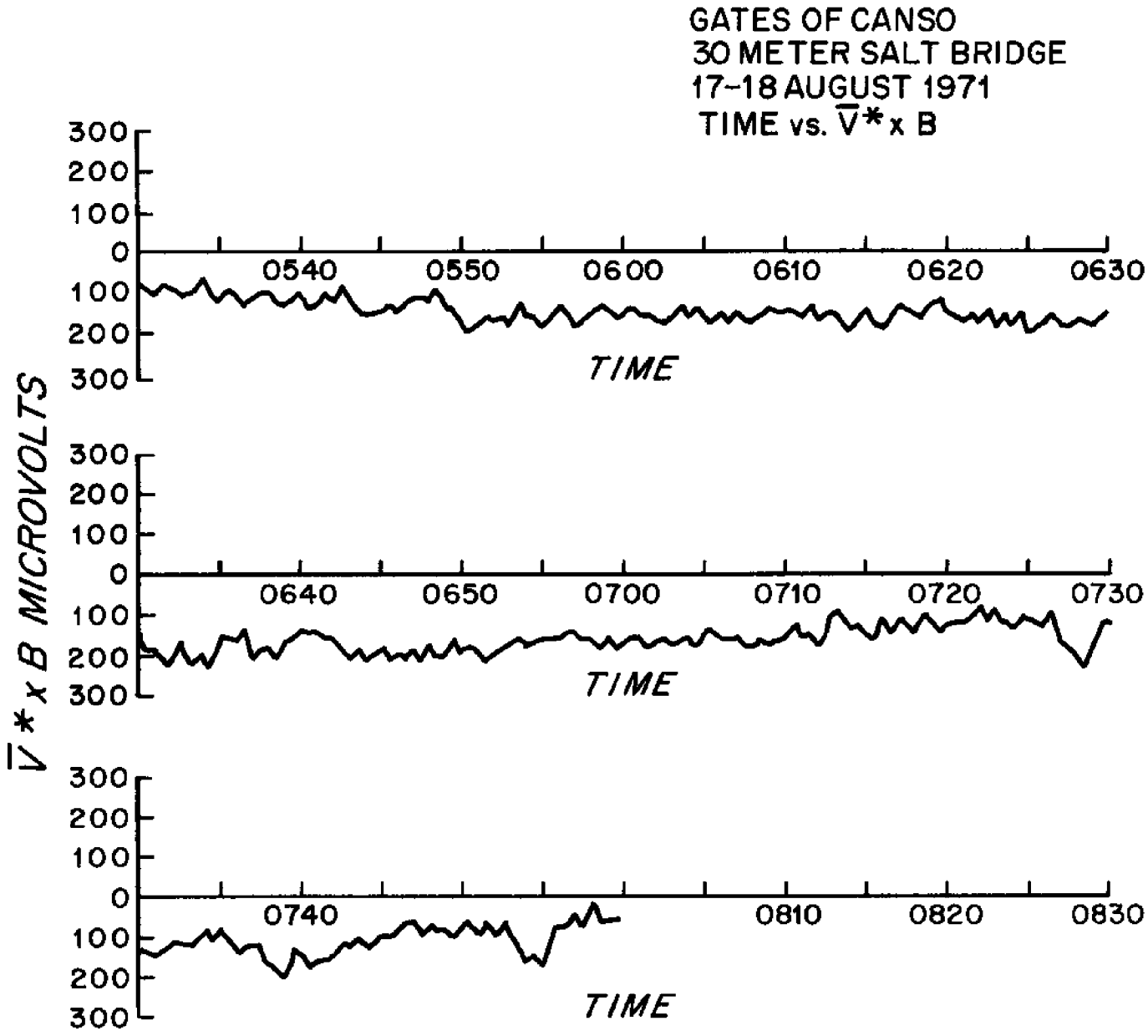

Figure 40. Gates of Canso 0530-0800.

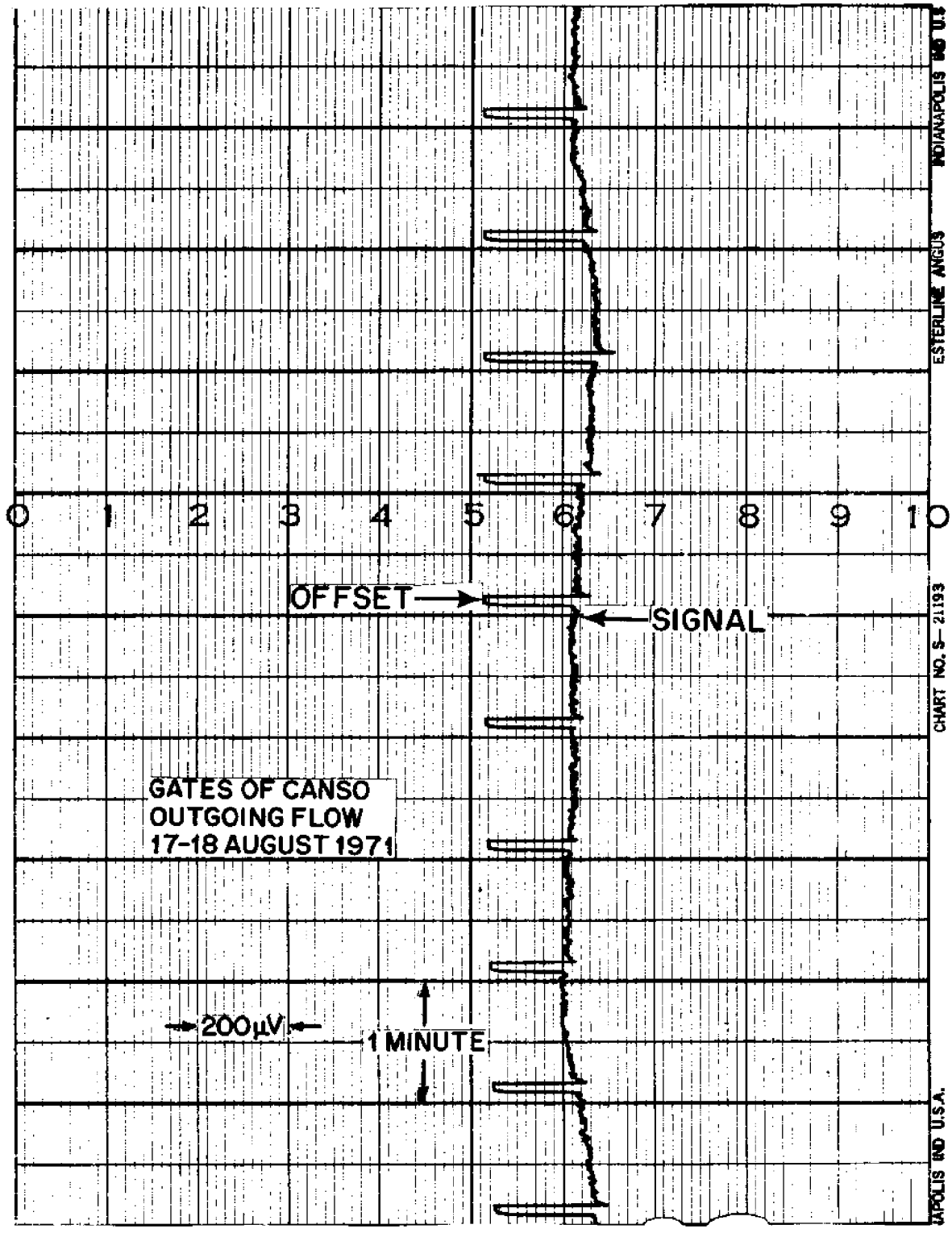

Figure 41. Typical Data-Gates of Canso Outgoing Flow.

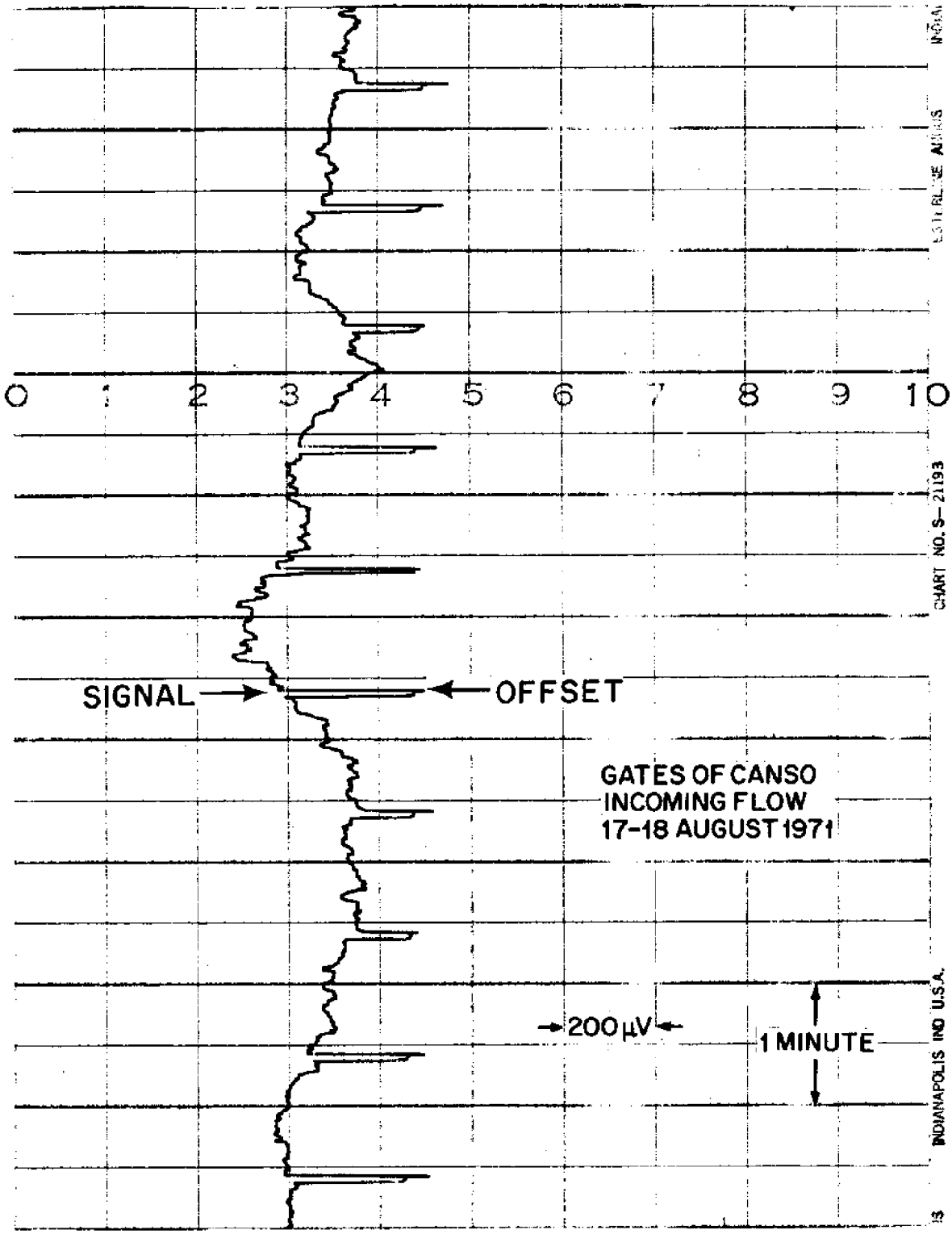

Figure 42. Typical Data-Gates of Canso Incoming Flow.

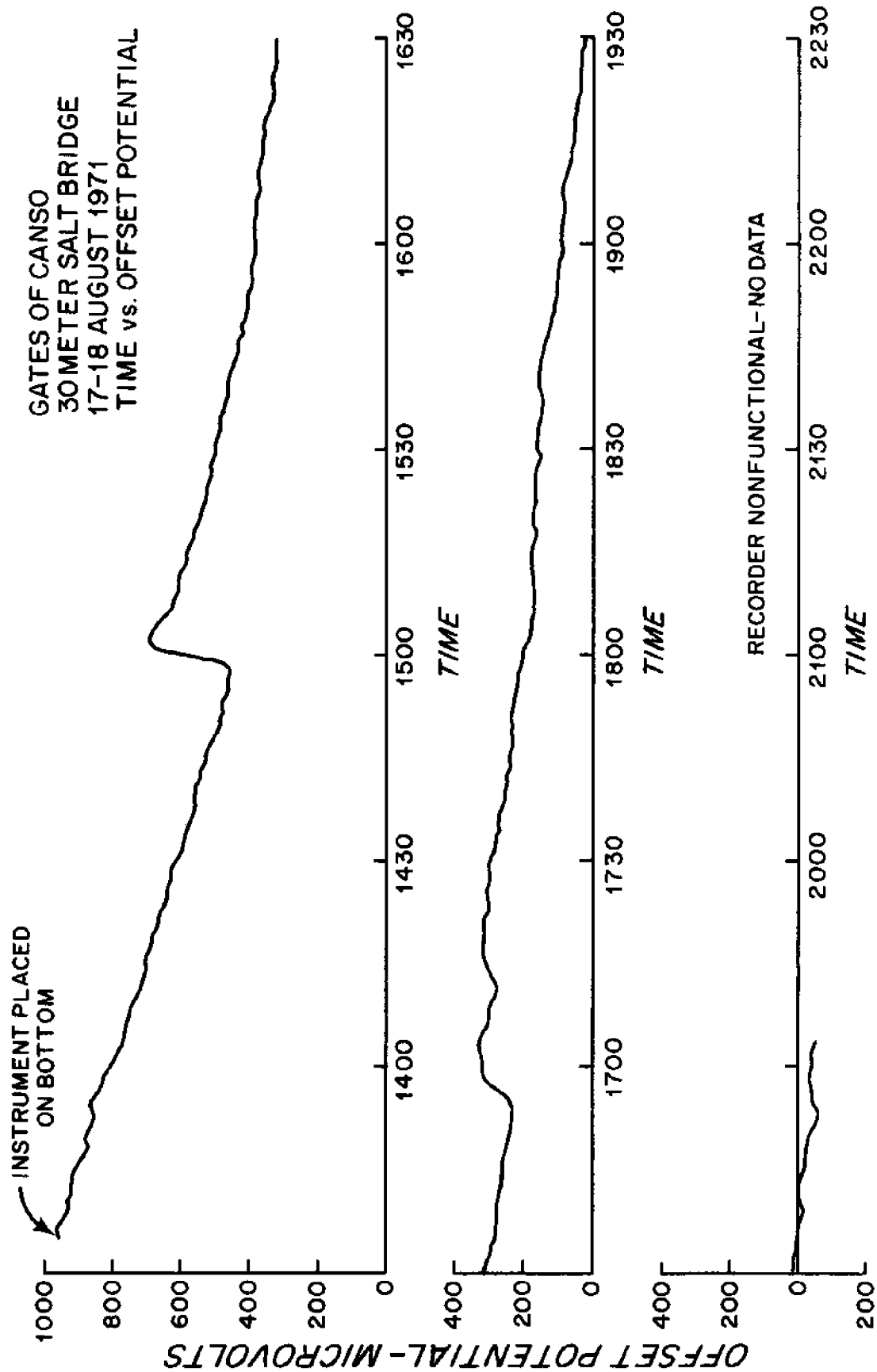

Figure 43. Offset Potential Drift-Gates of Canso 1330-2230.

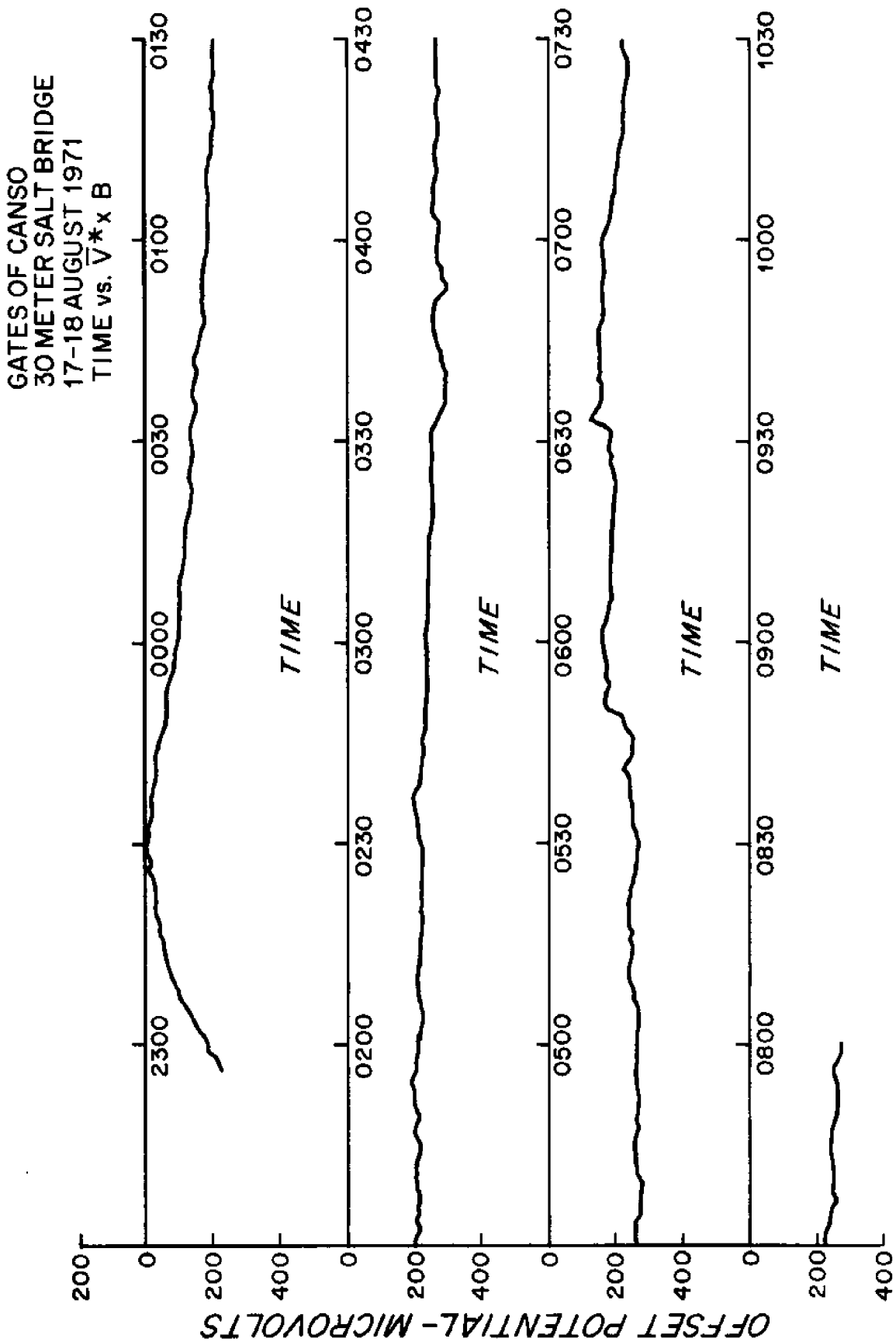

Figure 44. Offset Potential Drift-Gates of Canso 2230-0800.

.26 knots). Using this value in converting the data from the Gate of Canso, we obtain an average flow of .26 to .52 knots. This flow does not agree with what was expected. It was anticipated that a much higher flow would be obtained. A speedometer aboard the anchored R.V. SHADOWFAX measured currents in excess of 4 knots at times. This difference can be explained if - (A) the assumptions in Appendix 2 are incorrect, or (B) the average flow through the gate is, indeed, between .26 and .52 knots, and our original assumptions concerning this flow are in error.

These assumptions used in Appendix 2 appear to be good. Malkus and Stern (1952) used the same approximations with good results. Therefore, it appears that the assumption concerning the flow is in error. It was assumed that the current was approximately uniform throughout the depth of the channel in the vicinity of the deployed GEK. It is now believed that there is only a thin tongue of current that moves through the Gate with relatively quiet water or countercurrents in other regions.

APPENDIX 1

AMPLIFIER OPERATION IN NORMAL AND SWITCHED MODES.

Let: x = potential of electrode in short salt bridge

y = offset potential between electrodes

z = true signal

Normal Operation

x + y + z = potential of electrode in long salt bridge with respect to electrode in short salt bridge.

First amplifier stage: $V_{out} = 250(x + y + z)$

Second amplifier stage: $V_{out} = [x - 250(x + y + z)]20$

$V_{out} = -(4980x + 5000y + 5000z)$

Solenoids Activated

x + y = potential of electrode normally in long salt bridge w.r.t. other electrode.

First amplifier stage: $V_{out} = 250(x + y)$

Second amplifier stage: $V_{out} = [x - 250(x + y)]20$

$V_{out} = -(4980x + 5000y)$

Therefore: Amplified true signal = V_{out} (normal) - V_{out} (activated)

Amplified true signal = -5000z

APPENDIX 2

CONVERSION FACTOR FROM VOLTAGE TO CURRENT SPEED.

Towed behind ASTERIAS: 20 meter salt bridge

$$E = (V - \overline{V}^*) \times F$$

$$F_z = 0.5 \text{ gauss} = 0.5 \times 10^{-4} \text{ webers/meter}^2$$

Assuming a 100 microvolt signal, then:

$$E = 100 \times 10^{-6} \frac{\text{volts}}{20 \text{ meter}} = 5 \times 10^{-6} \frac{\text{volts}}{\text{meter}}$$

$$V - \overline{V}^* = \frac{5 \times 10^{-6} \text{ volts/meter}}{.5 \times 10^{-4} \text{ webers/meter}^2}$$

$$V - \overline{V}^* = .1 \text{ meter/sec}$$

Therefore: $V - \overline{V}^*$ is approximately .2 knots

Bottom Mounted at Gate of Canso: A complete analysis of the electric currents flowing in the Gate of Canso depends on the exact velocity distribution and bathymetry. It is not intended here to do such an analysis but rather to derive an approximate conversion from measured voltage to velocity through the Gate. To simplify the calculation, two models will be used: the first to express the geometry in the simplest way and the second to simplify the field calculation.

The width of the channel, the depth of the water, and the average velocity of the water are the simplest parameters which can be assumed for the Gate of Canso. So let us represent the Gate as a rectangular channel of great length, width L and depth d. The channel is filled with water of resistivity ρ_w moving at a uniform velocity V normal to a vertical magnetic field B. The bottom has a uniform resistivity ρ_B and extends to infinity in the lower half space (below the water surface).

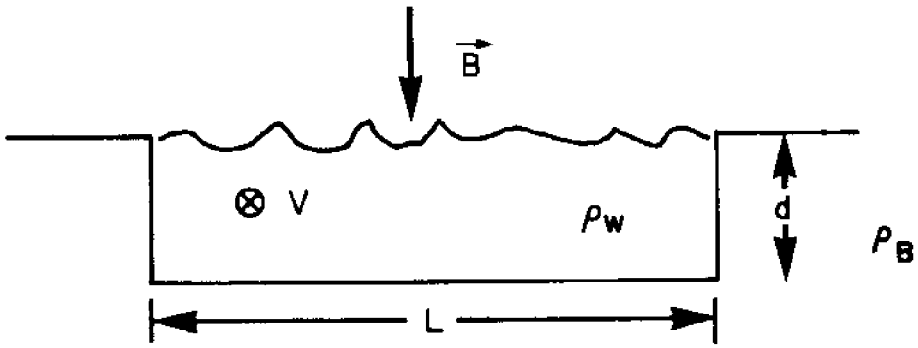

d = depth

L = Length

We wish to find the voltage between the lower corners of this channel as a function of the velocity. In the idealization of the Gate which we have assumed, there is a distribution of potential along the sides and bottom of the channel which arises from the geomagnetic electro-kinetic field and from

the electric current distribution in the sediment and the water. A great simplification can be made by assuming the side walls of the channel are conducting cylinders half immersed in the sediment, and the water in the channel is replaced by an emf $\vec{E} = \vec{V} \times \vec{B}$ in series with a resistance $R_w = \rho_w L/d$ per unit length. This model is easy to solve and is an approximation to the first model if the dimensions are chosen suitably. A schematic configuration of a unit length of this second model is shown below.

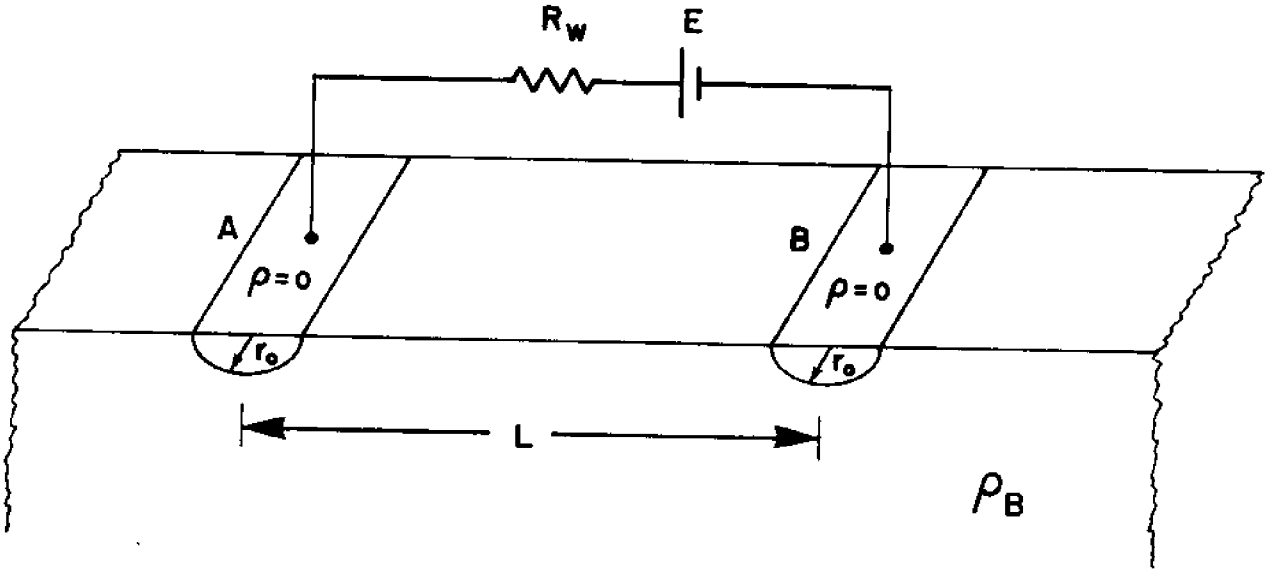

To scale the second model to the first, the immersed circumference of the cylinders is made equal to the depth of the channel plus a portion of the bottom width, say a quarter of L. Thus $r_o = (d+L/4)/\pi$. It can be noted that the resistance through the sediment between A and B is just twice what it would be between two full cylinders of radius r_o separated by L in a full space of sediment with resistivity ρ_B. The full cylinders in a full space of sediment are symmetric and the resistance per unit length between them can be calculated.

$$R_{\text{Full Space}} \approx 2\rho_B \int_{r_o}^{L} \frac{dr}{2\pi r} \quad \text{if } L >> r_o$$

$$R_B = 2R_{\text{Full Space}} \approx 2\left[\frac{\rho_B}{\pi} \ln(L/r_o)\right]$$

$$R_B \approx \frac{2\rho_B}{\pi} \ln[\pi L/(d+L/4)]$$

Then the voltage across the channel will be $E_m = ER_B/(R_B+R_w)$

At the Gate of Canso, L = 30 meters, d = 5 meters, $\rho_B = 4\rho_w$.

$$R_B = 1.3\rho_B = 5.2\rho_w$$

$$R_w = 6.0\rho_w$$

$$E_m = .46E$$

Therefore, 1/2 of our voltage drop occurs in the sediment. This can be included in the expression for measured voltage as a K factor

$$K \cdot E_{\text{measured}} = \overline{V}^* \times B \text{ where } K = 2.$$

Assuming a 100 microvolt signal, it follows that:

$$E = 100 \times 10^{-6} \text{ volts}/30 \text{ meters} = 3.33 \times 10^{-6} \text{ volts/meter}$$

$$\overline{V}^* = \frac{2 \cdot 3.33 \times 10^{-6} \text{ volts/meter}}{.5 \times 10^{-4} \text{ webers/m}^2}$$

$\overline{V}^* = 2 \cdot 6.67$ cm/sec, which is approximately .26 knots.

SELECTED ANNOTATED BIBLIOGRAPHY

1. Drever, R.G., and Sanford, T.B., "A Free-Fall Electromagnetic Current Meter - Instrumentation," Proceedings of the I.E.R.E. Conference on Electronic Engineering in Ocean Technology, I.E.R.E., 8-9 Bedford Square, London, 1970, pp. 353-370.

This paper describes the instrumentation and operation of the free-fall electromagnetic current meter. The theory of operation is only briefly discussed. The instrument measures the electric fields induced in the unit and in the sea due to motion through the geomagnetic field. The horizontal velocity of the instrument is governed by the local horizontal velocity of the ocean. It is assumed that the instrument, at all depths, is in equilibrium with the horizontal motion of the sea. The technique used by the authors is capable of rapidly measuring the variations of horizontal velocity as a function of depth with a precision below 1 cm/sec. The essential difference between this instrument and the surface towed Geomagnetic Electro-Kinetograph (GEK) is that the former is used at the sea surface to study the horizontal structure of an ocean current while the free-fall instrument is used to study the vertical structure. The main objective for developing the free-fall instrument was to determine if it was feasible to measure the weak motionally induced electric fields in the ocean currents. The tests showed that it was not only practical but very useful oceanographically to make these measurements.

2. Longuet-Higgins, M.S., Stern, M.E., and Stommel, H., "The Electric Field Induced by Ocean Currents and Waves, with Applications to the Method of Towed Electrodes," Papers in Physical Oceanography and Meteorology, Vol. 13, No. 1, M.I.T. and Woods Hole Oceanographic Inst., Nov., 1954, pp. 1-37.

This is an extended discussion of the basic principles underlying the nature of the electric field induced in the ocean by particular types of velocity distribution. A fundamental difficulty in the problem is that the electrical field at any point depends not only on the local water velocity, but also on the electrical current-density, which is determined

to a greater or less extent by the whole velocity field. The principle of induction and the theory of towed electrodes is set out in detail. The field equations necessary for an exact analysis are given but particular solutions for the cases of a sinusoidal stream, and streams of rectangular and elliptical cross-section are worked out in detail. The solution for the rectangular section is of special interest, since it can be used to build up the solution for a stream of arbitrary cross-section, to any degree of approximation.

3. Malkus, W.V.R., and Stern, M.E., "Determination of Ocean Transports and Velocities by Electromagnetic Effects," Sears Foundation: Journal of Marine Research, Vol. 11, No. 2, November 15, 1952, pp. 97-105.

The electric potentials in and about an ocean current are shown by the authors to be directly related in a simple fashion to the total fluid transport. Several techniques of measurement are discussed, including the Geomagnetic Electro-Kinetograph method. The errors that may be involved in each case are also discussed. Their work determines the relation between the total potentials across the current and the total volume transport of fluid. The approximations involved in relating local electric observables to local velocities are also determined.

4. Sanford, Thomas B., "Motionally Induced Electric and Magnetic Fields in the Sea," Journal of Geophysical Research, Vol. 76, No. 15, May 20, 1971, pp. 3476-3492.

Motionally induced electric and magnetic fields are investigated in the sea, crust, and mantle for large-scale low-frequency oceanic flows. Dr. Sanford shows that three-dimensional flows generate large-scale horizontal electric currents not present in two-dimensional motions. He further shows that the variable $\overline{V}^*$, the conductivity-weighted, vertically averaged velocity is important in the generation of both local and large-scale electric currents. Expressions are derived showing that $\overline{V}$, the vertically averaged velocity, can be determined for measurements of the

induced electric and magnetic fields at the sea floor. Several special cases are calculated illustrating the influences of the mantle, the conducting sediments, and the horizontal scales of the motion. The three-dimensional theory was developed because the two-dimensional theory is generally inadequate when applied to actual flows having variations in time and space.

5. von Arx, William S., "An Electromagnetic Method for Measuring the Velocities of Ocean Currents From a Ship Under Way," Papers in Physical Oceanography and Meteorology, Vol. 11, No. 3, M.I.T. and Woods Hole Oceanographic Inst., March, 1950, pp. 1-62.

This paper briefly traces the general development of the Geomagnetic Electro-Kinetograph starting from Faraday's original suggestion and early experiments in 1832. A general discussion of the basic principles is given but the main content of the paper deals with the author's surface-towed Geomagnetic Electro-Kinetograph (GEK). Practical considerations and the validity of the electromagnetic method are presented to the reader. Application of the electromagnetic method to observations in shoal water, including both observations while under way and at a fixed station, are also discussed by the author.

6. Runcorn, S., "Measurements of Planetary Electric Currents," Nature, Vol. 202, 1964, pp. 10-13.

7. Stommel, H., "Exploratory Measurements of Electric Potential Differences between Widely Spaced Points in the North Atlantic Ocean," Archiv fur Meteorologie, Geophysik und Bioklimatologie, 7, Ser. A, 1954, pp. 292-304.

8. Young, F.B., H. Gerrard, and W. Jevons, "On Electrical Disturbances Due to Tides and Waves," Phil. Mag. Ser. 6, Vol. 40, 1920, pp. 149-159.